



A comprehensive analysis of the $B^0 \rightarrow K^{*0} \mu^+ \mu^-$ decay

LHCb collaboration[†]

Abstract

An analysis of the $B^0 \rightarrow K^{*0}(\rightarrow K^+\pi^-)\mu^+\mu^-$ decay is presented using proton-proton collision data collected by the LHCb experiment, corresponding to an integrated luminosity of 8.4 fb^{-1} . The full set of CP -averaged and CP -asymmetric angular observables is determined in bins of the invariant mass squared of the dimuon system, as well as the branching fraction relative to the $B^0 \rightarrow J/\psi(\rightarrow \mu^+\mu^-)K^+\pi^-$ decay. For the first time, the full set of observables pertaining to the $K^+\pi^-$ S-wave contribution to the final state are presented and consideration is given to effects arising from the mass of the muons. The measurements of the CP -averaged observables and the branching fractions continue to exhibit the pattern of tensions with the Standard Model predictions that have been seen in previous analyses that use part of the dataset considered in this study. The extracted CP -asymmetry observables show no significant deviations from zero.

Submitted to Phys. Rev. Lett.

© 2025 CERN for the benefit of the LHCb collaboration. CC BY 4.0 licence.

[†]Authors are listed at the end of this paper.

An intriguing set of discrepancies between experimental measurements and the predictions of the Standard Model (SM) has been observed in the $B^0 \rightarrow K^{*0} \mu^+ \mu^-$ decay [1–6] and in several other processes mediated by the same underlying $b \rightarrow s \mu^+ \mu^-$ quark transition [7–10]. In the SM, these flavour-changing neutral currents occur only via virtual quantum loops. The resulting suppression means that as yet undiscovered particles, which could have masses that make them inaccessible to direct searches, may contribute to these decays at a level comparable to the SM processes. For example, tensions with SM predictions may be explained by New Physics models that introduce an additional contribution to the effective four-fermion $bs\mu\mu$ vector coupling, \mathcal{C}_9 [11–19]. However, despite numerous theoretical developments [20–37], there is still debate about whether the observations might instead be explained by SM long-distance effects [11, 16, 18, 20, 24, 34, 38–43]. Recent LHCb analyses that try to quantify these effects by fitting $B^0 \rightarrow K^{*0} \mu^+ \mu^-$ data together with ancillary data and theoretical predictions do not suggest substantially enhanced long-distance effects [44, 45].

This Letter presents the most precise measurements to date of the CP -averaged angular observables of the $B^0 \rightarrow K^{*0} \mu^+ \mu^-$ decay, the associated CP asymmetries and the differential branching fraction. The K^{*0} resonance, where K^{*0} denotes the $K^*(892)^0$ meson, is reconstructed through its decay to $K^+ \pi^-$. This final state receives contributions from decays with the $K^+ \pi^-$ in an S-wave configuration, as well as the P-wave configuration from the K^{*0} . The reported observables correspond to averages over different regions of the dimuon invariant mass squared, q^2 . The dataset used corresponds to an integrated luminosity of 8.4 fb^{-1} of proton-proton collisions collected by the LHCb experiment during 2011, 2012, and 2016–2018. Throughout this Letter charge-conjugate processes are implied unless otherwise stated.

The analysis broadly follows the strategy of previous q^2 -binned studies of this decay mode, using LHCb data collected during 2011–2016 [1, 2, 5, 46–49]. The present study introduces several significant innovations over those earlier analyses. These include: an updated expression for interference effects in the differential decay rate; the first simultaneous treatment of all relevant kinematic variables for describing the decay, incorporating for the first time the invariant mass of the kaon-pion system, $m(K^+ \pi^-)$, which is also studied in a wider range than previously considered; the first treatment of the effect of lepton masses; the first simultaneous measurement of the differential branching fraction alongside the angular observables; and the first measurement of the full set of CP asymmetries. The inclusion of $m(K^+ \pi^-)$ directly when measuring the angular distributions gives sensitivity to new observables related to the interference between P- and S-wave contributions [50]. In this study effects associated with lepton masses are found to have an important impact across a range of q^2 values below the charmonium resonances. The approach taken for the simultaneous measurement of the differential branching fraction accounts for any variation of the angular decay rate due to potential New Physics contributions, while the first measurement of the full set of CP asymmetries is provided alongside the full covariance matrix relating the CP -averaged and CP -asymmetric observables. Narrower q^2 bins compared to those from previous analyses are included to gain an improved understanding of the q^2 dependence of the measured observables. The offline selection has also been reoptimised compared to the previous analysis [5]. Finally, the analysis described in this Letter was performed twice, using two independently developed frameworks, providing an important validation of the results.

The $B^0 \rightarrow K^+ \pi^- \mu^+ \mu^-$ decay is completely described by five kinematic variables:

q^2 , $m(K^+\pi^-)$, and the three decay angles, $\vec{\Omega} = (\cos\theta_\ell, \cos\theta_K, \phi)$ defined in Ref. [47]. The resulting differential decay rate is parameterised by approximately 20 CP -averaged angular observables, with a similar number describing the difference in angular distributions between B^0 and \bar{B}^0 decays (CP asymmetries). These observables are determined for candidates with $0.7459 < m(K^+\pi^-) < 1.0959 \text{ GeV}/c^2$, except for the $17 < q^2 < 19 \text{ GeV}^2/c^4$ region, where a narrower $0.7459 < m(K^+\pi^-) < 0.9590 \text{ GeV}/c^2$ range is applied. This differential rate is described in Ref. [50], with the specific form used for this analysis provided in the End Matter. Observables accessible in the $B^0 \rightarrow K^{*0}\mu^+\mu^-$ decay have previously been extensively studied [51–65]. The analysis presented here measures: the CP -averaged and CP -asymmetry observables, S_i and A_i , for both P-wave and S-wave, including the interference between the two; the P-wave decay rate; and the $P_i^{(\prime)}$ observables that are constructed to cancel the leading-order theoretical uncertainties from the $B^0 \rightarrow K^{*0}$ form factors [64].

As detailed in the End Matter, the total basis of observables may be reduced by making assumptions on the effect of the lepton mass, or the presence of New Physics scalar or tensor amplitudes. Without these assumptions, significant correlations between some observables can lead to sizeable biases or increased uncertainties in the measured quantities, meaning that a reduced model gives better precision on the extracted observables. Given the precision of this analysis, the effect of the muon mass is found to be significant up to $q^2 \approx 6 \text{ GeV}^2/c^4$, with the most pronounced effect at the lowest q^2 values. Therefore, for the first time, this analysis accounts for the lepton mass when determining the angular observables.

The LHCb detector is a single-arm forward spectrometer covering the pseudorapidity range $2 < \eta < 5$, described in detail in Refs. [66, 67]. The polarity of the LHCb dipole magnet is periodically reversed to cancel the effects of oppositely charged particles being deflected in opposite directions. The online event selection is performed by a trigger, which comprises a hardware stage, based on information from the calorimeter and muon systems, followed by a software stage [68]. Data selected by the trigger undergo a further, centralised, offline processing step [69].

Signal candidates are formed from a pair of oppositely charged tracks that are identified as muons, combined with a K^{*0} candidate that is formed from tracks identified as a kaon and a pion. The tracks of the final-state particles are required to have significant impact parameter with respect to all primary proton-proton interaction vertices (PVs) in the event and to form a common vertex of good quality. The B^0 -candidate decay vertex is required to be significantly displaced from all the PVs. It is also required that the angle between the reconstructed B^0 momentum and the vector connecting one of the PVs to the reconstructed B^0 decay vertex, θ_{DIRA} , is small.

Large samples of simulated events, produced with the software described in Refs. [70–72], are used to assess the reconstruction and selection efficiencies for signal candidates and to estimate the contamination from residual backgrounds. Inaccuracies in the simulation are corrected using control samples from data. The simulated particle-identification (PID) response is corrected using dedicated data control samples [73, 74], as is the track-reconstruction efficiency [75]. Data-simulation differences arising from mismodelled B^0 kinematics, event multiplicity, hardware trigger efficiency, track and vertex quality are corrected using two separate control modes; $B^0 \rightarrow J/\psi K^{*0}$ and $B^+ \rightarrow J/\psi K^+$. The results from the two modes are compared and found to be in good agreement, with the differences in the corrections used to evaluate a systematic uncertainty.

Residual backgrounds consist of a combinatorial component, formed from fragments of multiple decays, with distributions that vary smoothly in $m(K^+\pi^-\mu^+\mu^-)$, $m(K^+\pi^-)$ and $\vec{\Omega}$; and peaking backgrounds, where a single decay is selected but with some of the final-state particles misidentified or misreconstructed, which tend to accumulate in specific $m(K^+\pi^-\mu^+\mu^-)$ and $\vec{\Omega}$ regions. The combinatorial background is reduced by a dedicated boosted decision tree (BDT) classifier [76, 77]. The classifier is trained using $B^0 \rightarrow J/\psi K^{*0}$ candidates in the $8.0 < q^2 < 11.0 \text{ GeV}^2/c^4$ region with the background contribution statistically subtracted using the *sPlot* procedure [78]. For the background training sample, candidates with invariant mass $5.5 < m(K^+\pi^-\mu^+\mu^-) < 5.7 \text{ GeV}/c^2$ are used. Separate BDTs are trained using a cross-validation technique [79] for each of the three run periods (2011–2012, 2016, 2017–2018), which reflect significant changes in the data-taking conditions. The variables used as inputs to the BDT classifier include the reconstructed B^0 decay time and the vertex-fit quality, as well as its momentum, transverse momentum, and θ_{DIRA} . Additionally, PID information from the Ring Imaging Cherenkov detectors and the muon system, and variables describing the isolation of the final-state tracks [80], are used. A requirement is placed on the BDT output to maximise the significance of $B^0 \rightarrow K^{*0}\mu^+\mu^-$ signal decays. This requirement rejects more than 98% of the remaining combinatorial background, while retaining more than 89% of the signal.

Dedicated vetoes are applied to reduce peaking backgrounds from processes such as $B_s^0 \rightarrow \phi(1020)(\rightarrow K^+K^-)\mu^+\mu^-$, $A_b^0 \rightarrow pK^-\mu^+\mu^-$, $B^0 \rightarrow J/\psi K^{*0}$, $B^0 \rightarrow \psi(2S)K^{*0}$ and $\bar{B}^0 \rightarrow \bar{K}^{*0}\mu^+\mu^-$, where at least one final-state particle has been misidentified. The latter decay forms a background if both the kaon and pion are misidentified. The decays involving charmonia can mimic the signal decay if a muon is misidentified as a hadron and vice versa. The vetoes use the invariant mass of the candidates recomputed with appropriate changes in the particle mass hypotheses, and variables that combine PID and track information about the particle track in a neural network [73]. The $B^+ \rightarrow K^+\mu^+\mu^-$ decay can constitute a background if the final-state particles are combined with a random pion produced by other processes in the event. This background is vetoed by removing candidates with $m(K^+\pi^-\mu^+\mu^-) > 5.38 \text{ GeV}/c^2$ if they have a $K^+\mu^+\mu^-$ invariant mass within $\pm 0.06 \text{ GeV}/c^2$ of the known B^+ mass [81].

The analogous background due to $B^+ \rightarrow J/\psi K^+$ decays remains significant for $q^2 \gtrsim 6 \text{ GeV}^2/c^4$, owing to the long radiative tail of the J/ψ resonance and its large branching fraction to the dimuon final state. As a result of this radiative tail, these candidates have a $m(K^+\mu^+\mu^-)$ value below the known B^+ mass and so escape the veto for the $B^+ \rightarrow K^+\mu^+\mu^-$ background. A dedicated BDT classifier, trained using simulation to represent both the signal and this particular background, is used to suppress these candidates to a negligible level. Similarly, a background can occur from cascades of semileptonic decays with large branching fractions, *e.g.* $B \rightarrow \bar{D}(\rightarrow K^+\mu^-X)\mu^+X$, when incorrectly combined with a pion selected from elsewhere in the event. Here, X can represent any additional unreconstructed particles in the final state. Due to the inherent asymmetry of the momenta of the two muons, these decays lead to a characteristic asymmetry in $\cos\theta_\ell$. Another dedicated BDT classifier is trained to reduce these backgrounds to negligible levels. Data candidates with $m(K^+\pi^-\mu^+\mu^-) > 5.35 \text{ GeV}/c^2$, enriched in semileptonic contributions by requiring $m(K^+\mu^-) < 1.9 \text{ GeV}/c^2$ and $q^2 < 8.0 \text{ GeV}^2/c^4$, serve as a background proxy, while simulated candidates with $m(K^+\mu^-) < 1.9 \text{ GeV}/c^2$ are used as a signal proxy. The most discriminating variables include the difference in three-momenta between the K^{*0} candidate and dimuon pair and the transverse momentum of the pion.

The Cabibbo-suppressed background from $\bar{B}_s^0 \rightarrow K^{*0} \mu^+ \mu^-$ decays is expected to be at the level of 1% of the signal. The analysis is performed with and without this background component included in the fit, and the effect on the measured decay rate is found to be negligible. Backgrounds from b -hadron decays to fully hadronic final states, where two hadrons are misidentified as muons, are negligible. The residual contamination from peaking backgrounds is estimated to be at the level of 2% of the signal. Such backgrounds are not modelled in the analysis procedure and are considered only as a source of systematic uncertainty.

Candidates are required to have $5.17 < m(K^+ \pi^- \mu^+ \mu^-) < 5.70 \text{ GeV}/c^2$ and $0.7459 < m(K^+ \pi^-) < 1.0959 \text{ GeV}/c^2$. The larger $m(K^+ \pi^-)$ window used here compared to previous analyses increases the yield of S-wave signal candidates, which allows for a more precise determination of the S-wave fraction, F_S , and the observables pertaining to the interference of P- and S-wave amplitudes. Backgrounds from the decays $B^0 \rightarrow J/\psi(\rightarrow \mu^+ \mu^-) K^{*0}$, $B^0 \rightarrow \psi(2S)(\rightarrow \mu^+ \mu^-) K^{*0}$ and $B^0 \rightarrow \phi(1020)(\rightarrow \mu^+ \mu^-) K^{*0}$, which result in the same final state as the signal, are removed by rejecting candidates with q^2 in the ranges $8.0 < q^2 < 11.0 \text{ GeV}^2/c^4$, $12.5 < q^2 < 15.0 \text{ GeV}^2/c^4$ and $0.98 < q^2 < 1.10 \text{ GeV}^2/c^4$. The former two decays involve tree-level $b \rightarrow c\bar{c}s$ transitions and are used to validate several aspects of the analysis procedure.

An extended unbinned maximum-likelihood fit of the differential decay rate as a function of $m(K^+ \pi^-)$, the three decay angles, and $m(K^+ \pi^- \mu^+ \mu^-)$ is used to determine the angular observables and differential branching fraction relative to the normalisation mode $B^0 \rightarrow K^+ \pi^- J/\psi$ in each bin of q^2 . This five-dimensional approach introduces new interference observables [50] compared to previous iterations of this analysis and provides the optimal per-event sensitivity to the angular observables. The selected candidates are split into B^0 and \bar{B}^0 samples that are fit simultaneously, allowing for the full set of CP -averaged and CP -asymmetry observables to be extracted in a single fit, with all correlations determined. A model-independent measurement of both the relative branching fractions and the full set of CP -asymmetry observables is made by adding an extended term to the likelihood, which uses the fitted yields of B^0 and \bar{B}^0 events to constrain their respective signal decay rates. This model independence is achieved by calculating the efficiencies of the signal and normalisation modes through integrating the angular distributions of the fit probability density functions (PDFs). The data are further divided according to the three run periods described above, resulting in six distinct samples. These samples are fitted simultaneously with the angular observables and relative branching fraction shared.

The distortion of the $(\vec{\Omega}, m(K^+ \pi^-), q^2)$ distribution due to the detector acceptance and the selection is modelled with an acceptance function. This five-dimensional function is parameterised with Legendre polynomials L and coefficients c as

$$\varepsilon(\vec{\Omega}, q^2, m(K^+ \pi^-)) = \sum_{ijmno} c_{ijmno} L_i(\cos \theta_\ell) L_j(\cos \theta_K) L_m(\phi) L_n(q^2) L_o(m(K^+ \pi^-)), \quad (1)$$

and is computed using simulation. Owing to the rapid variation of the acceptance at low q^2 , which would require high-order polynomials, the acceptance function is split into two regions of q^2 , separated by the ϕ resonance at $q^2 \approx 1 \text{ GeV}^2/c^4$. In order to account for detection asymmetries, the acceptance function is obtained separately for B^0 and \bar{B}^0 decays, and is further split by the three run periods. A goodness-of-fit method using BDTs [82] is employed to ascertain the minimal polynomial orders needed to properly

describe the simulated events for each run period. The resulting acceptance functions are incorporated in the fit, either by directly including them in the PDF from Eq. 2 (see End Matter), or by taking the inverse of the acceptance function as per-event weights. The latter method is employed when the function varies strongly across the q^2 bin width.

Each of the six subsamples has an extended term in the likelihood, allowing the number of signal events to be determined. The yields are normalised to the inclusive $B^0 \rightarrow K^+\pi^- J/\psi (\rightarrow \mu^+\mu^-)$ decay mode, with the branching fraction taken from Ref. [83] and scaled by a correction factor derived from the measured amplitudes in Ref. [83] to account for the fraction of decays that fall within the $m(K^+\pi^-)$ window of this analysis. When accounting for the $J/\psi \rightarrow \mu^+\mu^-$ decay, this results in the normalisation branching fraction (\mathcal{B}) being

$$\mathcal{B}(B^0 \rightarrow K^+\pi^- J/\psi (\rightarrow \mu^+\mu^-))|_{0.7459 < m(K^+\pi^-) < 1.0959 \text{ GeV}/c^2} = (4.88 \pm 0.22) \times 10^{-5}.$$

The uncertainty on this branching fraction partially arises from the uncertainties on the measured amplitudes, which, due to the covariance matrix not being provided in Ref. [83], are treated as uncorrelated.

The extended term of each sample of the fit calculates the expected signal yield relative to the corresponding sample of the normalisation mode, and so effects from B^0 - \bar{B}^0 production and final-state detection asymmetries cancel. The total CP asymmetry of the $B^0 K^+\pi^- J/\psi$ decay is well-measured and consistent with zero [84]. The $B^0 \rightarrow K^+\pi^- J/\psi$ yields and efficiencies are determined in dedicated fits for each sample, using the same acceptance and fit functions.

The background distribution is modelled with Chebyshev polynomials of either first, second or fourth order in $\cos\theta_\ell$, $\cos\theta_K$, ϕ and $m(K^+\pi^-)$. The coefficients are allowed to vary in the fit and the resulting distribution is assumed to factorise between these variables and $m(K^+\pi^-\mu^+\mu^-)$. Furthermore, the shape of the background is assumed to be the same for the B^0 and \bar{B}^0 samples. These assumptions are verified using data with $m(K^+\pi^-\mu^+\mu^-) > 5.35 \text{ GeV}/c^2$.

The $m(K^+\pi^-)$ distribution of the signal is modelled with the amplitudes $\mathcal{BW}_P(m(K^+\pi^-))$ and $\mathcal{L}_S(m(K^+\pi^-))$ for the P- and S-wave components, respectively. The P-wave amplitude includes only the $K^*(892)^0$ resonance and is modelled using a relativistic Breit–Wigner function with mass and width taken from Ref. [81] and the standard Blatt–Weisskopf angular momentum factors [85]. Contributions from higher-mass spin-1 resonances are found to be negligible in the analysed $m(K^+\pi^-)$ region. The amplitude $\mathcal{L}_S(m(K^+\pi^-))$ is taken to be a LASS function [86, 87] with parameters determined from a fit to the $B^0 \rightarrow K^+\pi^- J/\psi$ decay mode, except for the range parameter of the LASS function, r , which is fixed to $1.7 (\text{GeV}/c)^{-1}$ [88]. The value of the scattering parameter, which is extracted from the fit to the $B^0 \rightarrow K^+\pi^- J/\psi$ decay mode, is fixed to $3.25 (\text{GeV}/c)^{-1}$ in the fit to the signal candidates. The barrier radius factor of the decaying K^{*0} meson is fixed to $2.12 (\text{GeV}/c)^{-1}$, a value again extracted from the fit to the $B^0 \rightarrow K^+\pi^- J/\psi$ decay mode. The analogous radius of the B^0 meson is fixed to $1.6 (\text{GeV}/c)^{-1}$ [89]. The signal shape in $m(K^+\pi^-\mu^+\mu^-)$ is modelled from simulation using the sum of two Crystal Ball functions [90] with tails to opposite sides, a common peak position, and width scaling factors accounting for differences between data and simulation derived from the $B^0 \rightarrow K^+\pi^- J/\psi$ fits. The combinatorial background is described by an exponential distribution in $m(K^+\pi^-\mu^+\mu^-)$.

Several fits of the data are performed with different angular observables floated, corresponding to different assumptions about the underlying physics. Making such assumptions reduces the number of observables, resulting in improved statistical behaviour and better precision. Allowing for massive leptons, as well as scalar and tensor amplitudes, results in 25 CP -averaged angular observables. This is referred to as the “fully massive” model. Due to the large number of correlated parameters, this model generally exhibits reduced statistical precision for the measurement of individual observables. Unless stated otherwise, the region $q^2 < 1.0 \text{ GeV}^2/c^4$ is always fitted using the fully massive model. If leptons are assumed to be massless, two relations between the angular observables can be imposed: $S_2^c = -S_1^c$ and $S_1^s = 3S_2^s$. This is referred to as the “massless” model. The relation $S_2^c = -S_1^c$ can introduce a bias for lower values of q^2 , as S_1^c has a dependence on the time-like amplitude that is suppressed by a factor of $\frac{4m_l^2}{q^2}$ [60]. Imposing only the relation $S_1^s = 3S_2^s$ removes this bias and is referred to as the “partially massive” model. This is discussed in more detail in the End Matter. A fit configuration is defined according to the model, q^2 binning scheme and whether S_i or $P_i^{(\prime)}$ angular observables are extracted. These observables differ in their normalisation, which is more complex for the $P_i^{(\prime)}$ case, see the End Matter and Ref. [64] for details. In total, six configurations are implemented:

- (i) Partially massive model, S_i basis, with CP asymmetries fixed to zero;
- (ii) Partially massive model, $P_i^{(\prime)}$ basis, with CP asymmetries fixed to zero;
- (iii) Fully massive model, S_i basis, with CP asymmetries fixed to zero;
- (iv) Massless model, S_i basis, with both CP -averaged and CP -asymmetry observables floated;
- (v) Massless model, applied also in the $q^2 < 1.0 \text{ GeV}^2/c^4$ region, P_i basis, with CP asymmetries fixed to zero;
- (vi) Partially massive model, S_i basis, with CP asymmetries fixed to zero and q^2 bins with widths half the size of those in the other configurations.

Configuration (v) is included solely to enable comparison with Ref. [5].

Pseudoexperiments are carried out to assess whether the extracted central values from the fit are unbiased, and whether the corresponding confidence intervals exhibit correct coverage. Observables with a relative bias or over/underestimation of the statistical uncertainty of more than 10% are corrected using a classical Neyman construction to find the best estimates of the true central values and 68% intervals [91]. Due to background contributions and the large number of fit parameters, the signal PDF can become negative in some regions of fit-variable phase space. To mitigate this unphysical effect, pseudodata for the Neyman construction are generated from a set of angular observables chosen to be as close as possible to those obtained from the data fit, while ensuring a positive PDF. The values used for the angular observables in the pseudoexperiment generation are updated for every point in the confidence belt for a given observable of interest. The central value is defined as the point in the confidence belt where the median most closely matches the fit result from data for the observable of interest. The positive PDFs are obtained with two methods: one varies the angular observables independently and tests whether the PDF is positive by sampling from the resulting angular model; the other

varies the underlying decay amplitudes and subsequently infers the values of the angular observables from the result. Both methods use a random walk to minimise the Euclidean distance between the resulting positive PDF and the PDF obtained from the fit to data. The difference in the resulting intervals and biases from the two methods is assigned as a systematic uncertainty. The results with and without these coverage and bias corrections are reported in the HEPDATA page.

The data are analysed using two independent implementations of the PDF and data-simulation corrections from different control modes. Both frameworks give compatible results when fitting pseudoexperiments and data, with residual discrepancies attributed to variations in the acceptance function, accounted for by systematic uncertainties, or to differences in the $B^+ \rightarrow K^+ \mu^+ \mu^-$ veto. Given the good level of agreement between the two approaches, the baseline framework was chosen randomly.

The fit results are found to have no significant dependence on run period, PID response, magnet polarity or the requirements made on the BDTs trained to reject the combinatorial and semileptonic backgrounds. The signal decay rate that results from the measured observables is also found to respect the symmetry relations given in Ref. [50]. The same BDT goodness-of-fit method from the fit of the acceptance simulation is used, as well as a point-to-point dissimilarity method [92], to check that the fit to the data is of good quality.

Systematic uncertainties on the observables are estimated using pseudoexperiments. A wide range of variations of the model used to generate these pseudoexperiments is considered, including the variation of relevant nuisance parameters, acceptance parameterisations, alternative fit model parameterisations, and injection of background events. The systematic uncertainties for all configurations are documented in the HEPDATA page. The dominant systematic uncertainty depends on the observable and q^2 bin in question. For the P- and S-wave observables the systematic uncertainties are generally less than 25% relative to the corresponding statistical uncertainties. At low q^2 the leading systematic uncertainties typically arise from the hardware trigger correction, from residual peaking background contamination and from the choice of polynomial orders in the angular background model. For the S-wave and interference observables, the modelling of the S-wave lineshape in $m(K^+ \pi^-)$ gives rise to the dominant systematic uncertainty and is often similar to or larger than the statistical uncertainty. Effects arising from a $K^+ \pi^-$ system in D-wave and higher partial-wave states are confirmed to be negligible in the analysed $m(K^+ \pi^-)$ region. For the relative P-wave branching fraction, the dominant uncertainty is due to the residual backgrounds for the normalisation mode.

The systematic uncertainties are evaluated coherently across all the q^2 bins. Therefore, the full covariance matrix of all observables across all bins is presented for use in subsequent phenomenological analyses. This is particularly pertinent for the large systematic uncertainty arising from the uncertainty on the branching fraction of the normalisation mode and, for the interference observables, the large systematic uncertainties arising from the choice of S-wave lineshape.

The CP -asymmetry observables all agree with SM expectations, with no significant CP asymmetry in the rate or angular observables. The CP -averaged observables S_2^c , A_{FB} , P_5' and $d\mathcal{B}/dq^2$ that are obtained from the fit configurations (i) and (ii) are shown together with their respective SM predictions in Fig. 1. In the approximation of massless leptons, the longitudinal polarisation fraction F_L is equivalent to $-S_2^c$. The results for all observables from all fit configurations are given in the HEPDATA page. Different

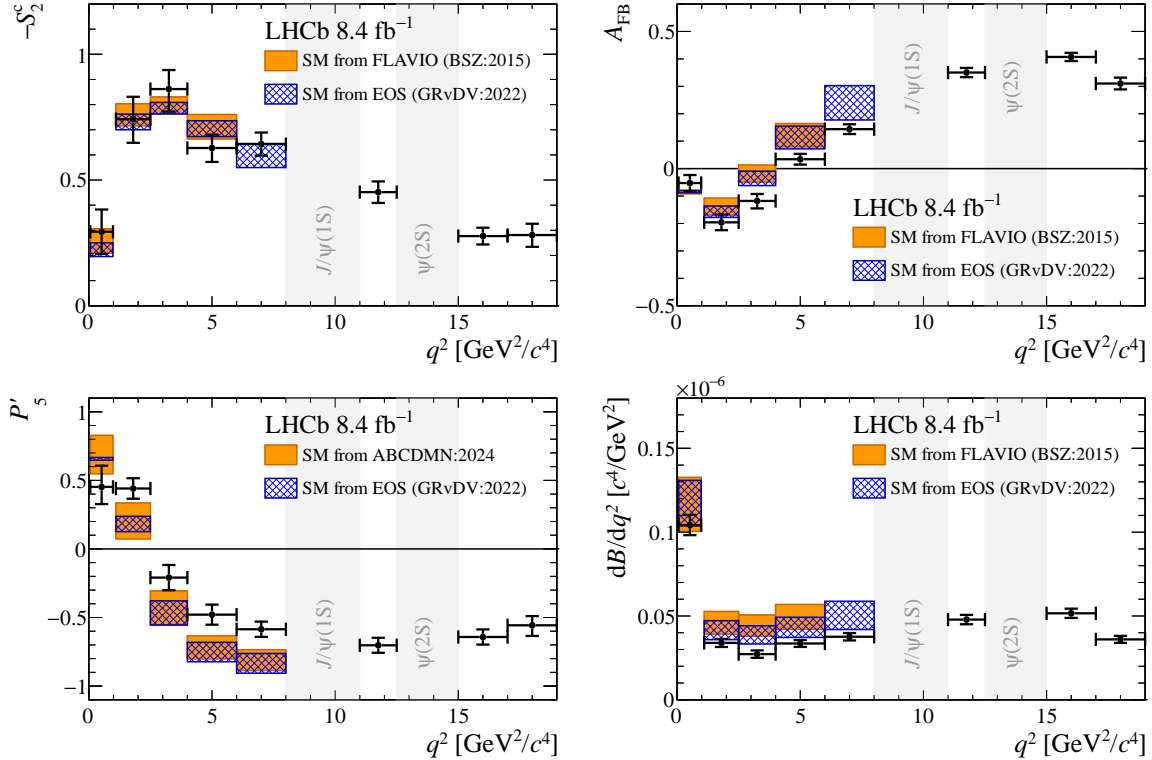


Figure 1: Results for the CP -averaged angular observables $-S_2^c$, A_{FB} and $d\mathcal{B}/dq^2$ from fit configuration (i), and P_5' from fit configuration (ii), in bins of q^2 . In the approximation of massless leptons, $-S_2^c$ is equivalent to the longitudinal polarisation fraction F_L . The data are compared to the SM predictions described in the text. The error bars show the total uncertainties.

SM predictions are also shown, obtained using: the FLAVIO package [93], where local form factors and long-distance effects are parameterised according to Ref. [27] (BSZ) and Ref. [13], respectively; the EOS package [94], where form factors are taken from Ref. [25,31,95] (GRvDV); or directly from Ref. [19] (ABCDMN). Taking into account the overlap between the data samples, the results of the fit configuration (v) are in excellent agreement with those reported in Ref. [5].

Considering the observables individually, the results are largely in agreement with the SM predictions. However, tensions with SM predictions in localised regions of phase space have broadly increased relative to the levels reported in Ref. [5]. The P_5' observable in the $4.0 < q^2 < 6.0 \text{ GeV}^2/c^4$ and $6.0 < q^2 < 8.0 \text{ GeV}^2/c^4$ bins is discrepant with the the GRvDV (ABCDMN) predictions at 2.6 and 2.7 standard deviations (σ) (2.1 and 2.4σ), respectively. Additionally, P_5' is in tension with the same predictions in the $1.1 < q^2 < 2.5 \text{ GeV}^2/c^4$ bin at the level of 2.7σ (1.6σ). The forward-backward asymmetry, A_{FB} , shows discrepancies with the BSZ (GRvDV) SM predictions in the $2.5 < q^2 < 4.0 \text{ GeV}^2/c^4$ and $4.0 < q^2 < 6.0 \text{ GeV}^2/c^4$ bins, with tension at the level of 2.5 and 1.9σ (2.2 and 1.7σ). The differential branching fraction is also 2.1σ (1.5σ) below the BSZ (GRvDV) SM predictions when considered in the q^2 bin $1.1 < q^2 < 6.0 \text{ GeV}^2/c^4$.

The FLAVIO [93] and EOS [94] software packages are used to fit the configuration (i) results, varying the parameter $\mathcal{R}e(\mathcal{C}_9)$. For the FLAVIO package, the default values of

the SM nuisances are used, including QCD effects as in Ref. [13,27], while for the EOS package, values are taken from Ref. [95]. The 3.3σ discrepancy with respect to the SM value of $\mathcal{R}e(\mathcal{C}_9)$ obtained with FLAVIO in Ref. [5] becomes 3.6σ (3.8σ) with FLAVIO (EOS). Including the differential branching fraction, the discrepancy increases to 4.1σ (4.0σ). Neglecting the $6.0 < q^2 < 8.0 \text{ GeV}^2/c^4$ bin that is closest to the charmonium resonances reduces the observed significance of $\mathcal{R}e(\mathcal{C}_9)$ by about 0.2σ . The best fit to the angular distribution is obtained with a shift in the SM value of $\mathcal{R}e(\mathcal{C}_9)$ by $-0.94_{-0.17}^{+0.21}$ (-0.92 ± 0.23) with FLAVIO (EOS). When combining the information from the angular observables with the branching fraction, a shift in $\mathcal{R}e(\mathcal{C}_9)$ of $-0.93_{-0.16}^{+0.18}$ (-0.94 ± 0.22) is obtained with FLAVIO (EOS). Differences between these numbers and those reported in Refs. [44,45], which fit for the Wilson coefficients directly, are due to the model inputs used, including the use of LHCb data to constrain the size of nonlocal contributions.

In summary, using proton-proton collision data collected by the LHCb experiment corresponding to an integrated luminosity of 8.4 fb^{-1} , the rare flavour-changing neutral-current decay $B^0 \rightarrow K^{*0} \mu^+ \mu^-$ has been analysed. For the first time, this analysis reports the complete set of interference observables between the $K^+ \pi^-$ P- and S-wave contributions, accounts for lepton mass effects and makes measurements in narrow q^2 bins and determines the branching fraction without depending on a model of the angular distribution. The complete set of CP asymmetries is determined and found to be consistent with zero. The results show a significant deviation from SM predictions [13,27,93,94] for the CP -averaged observables.

Acknowledgements

We express our gratitude to our colleagues in the CERN accelerator departments for the excellent performance of the LHC. We thank the technical and administrative staff at the LHCb institutes. We acknowledge support from CERN and from the national agencies: ARC (Australia); CAPES, CNPq, FAPERJ and FINEP (Brazil); MOST and NSFC (China); CNRS/IN2P3 (France); BMBWF, DFG and MPG (Germany); INFN (Italy); NWO (Netherlands); MNiSW and NCN (Poland); MCID/IFA (Romania); MICIU and AEI (Spain); SNSF and SER (Switzerland); NASU (Ukraine); STFC (United Kingdom); DOE NP and NSF (USA). We acknowledge the computing resources that are provided by ARDC (Australia), CBPF (Brazil), CERN, IHEP and LZU (China), IN2P3 (France), KIT and DESY (Germany), INFN (Italy), SURF (Netherlands), Polish WLCG (Poland), IFIN-HH (Romania), PIC (Spain), CSCS (Switzerland), and GridPP (United Kingdom). We are indebted to the communities behind the multiple open-source software packages on which we depend. Individual groups or members have received support from Key Research Program of Frontier Sciences of CAS, CAS PIFI, CAS CCEPP, Minciencias (Colombia); EPLANET, Marie Skłodowska-Curie Actions, ERC and NextGenerationEU (European Union); A*MIDEX, ANR, IPhU and Labex P2IO, and Région Auvergne-Rhône-Alpes (France); Alexander-von-Humboldt Foundation (Germany); ICSC (Italy); Severo Ochoa and María de Maeztu Units of Excellence, GVA, XuntaGal, GENCAT, InTalent-Inditex and Prog. Atracción Talento CM (Spain); SRC (Sweden); the Leverhulme Trust, the Royal Society and UKRI (United Kingdom).

End Matter

A The $B^0 \rightarrow K^+ \pi^- \mu^+ \mu^-$ differential decay rate

The decay may proceed via P- or S-wave amplitudes (higher partial waves are negligible in the $m(K^+ \pi^-)$ region analysed). The angular basis is described in Ref. [47]. The differential decay rate, described in Ref. [50], for \bar{B}^0 (B^0) is

$$\begin{aligned}
& \frac{1}{d(\Gamma + \bar{\Gamma})/dq^2} \Big|_{\text{P+S}} \frac{d^5 \bar{\Gamma}}{dq^2 dm_{K\pi} d\cos\theta_\ell d\cos\theta_K d\phi} \\
&= (1 - \hat{F}_S) \frac{9}{64\pi} \left[\zeta_1^s \sin^2 \theta_K + \zeta_1^c \cos^2 \theta_K + \zeta_2^s \sin^2 \theta_K \cos 2\theta_\ell + \zeta_2^c \cos^2 \theta_K \cos 2\theta_\ell \right. \\
&+ \zeta_3 \sin^2 \theta_K \sin^2 \theta_\ell \cos 2\phi + \zeta_4 \sin 2\theta_K \sin 2\theta_\ell \cos \phi + \zeta_5 \sin 2\theta_K \sin \theta_\ell \cos \phi \\
&+ \zeta_6^s \sin^2 \theta_K \cos \theta_\ell + \zeta_6^c \cos^2 \theta_K \cos \theta_\ell + \zeta_7 \sin 2\theta_K \sin \theta_\ell \sin \phi \\
&+ \left. \zeta_8 \sin 2\theta_K \sin 2\theta_\ell \sin \phi + \zeta_9 \sin^2 \theta_K \sin^2 \theta_\ell \sin 2\phi \right] \times |\mathcal{B}\mathcal{W}_P(m_{K\pi})|^2 \\
&+ \frac{1}{8\pi} \left[\left(\tilde{\zeta}_{1a}^c + \tilde{\zeta}_{2a}^c \cos 2\theta_\ell \right) \times |\mathcal{L}_S(m_{K\pi})|^2 \right. \\
&+ \frac{1}{2} \cos \theta_K \left(\tilde{\zeta}_{1b}^{c,\text{re}} \mathcal{R}e[\mathcal{L}_S(m_{K\pi})\mathcal{B}\mathcal{W}_P^*(m_{K\pi})] - \tilde{\zeta}_{1b}^{c,\text{im}} \mathcal{I}m[\mathcal{L}_S(m_{K\pi})\mathcal{B}\mathcal{W}_P^*(m_{K\pi})] \right) \\
&+ \frac{1}{2} \cos \theta_K \cos 2\theta_\ell \left(\tilde{\zeta}_{S1}^{\text{re}} \mathcal{R}e[\mathcal{L}_S(m_{K\pi})\mathcal{B}\mathcal{W}_P^*(m_{K\pi})] - \tilde{\zeta}_{S1}^{\text{im}} \mathcal{I}m[\mathcal{L}_S(m_{K\pi})\mathcal{B}\mathcal{W}_P^*(m_{K\pi})] \right) \\
&+ \frac{1}{2} \sin \theta_K \sin 2\theta_\ell \cos \phi \left(\tilde{\zeta}_{S2}^{\text{re}} \mathcal{R}e[\mathcal{L}_S(m_{K\pi})\mathcal{B}\mathcal{W}_P^*(m_{K\pi})] - \tilde{\zeta}_{S2}^{\text{im}} \mathcal{I}m[\mathcal{L}_S(m_{K\pi})\mathcal{B}\mathcal{W}_P^*(m_{K\pi})] \right) \\
&+ \frac{1}{2} \sin \theta_K \sin \theta_\ell \cos \phi \left(\tilde{\zeta}_{S3}^{\text{re}} \mathcal{R}e[\mathcal{L}_S(m_{K\pi})\mathcal{B}\mathcal{W}_P^*(m_{K\pi})] - \tilde{\zeta}_{S3}^{\text{im}} \mathcal{I}m[\mathcal{L}_S(m_{K\pi})\mathcal{B}\mathcal{W}_P^*(m_{K\pi})] \right) \\
&+ \frac{1}{2} \sin \theta_K \sin \theta_\ell \sin \phi \left(\tilde{\zeta}_{S4}^{\text{re}} \mathcal{I}m[\mathcal{L}_S(m_{K\pi})\mathcal{B}\mathcal{W}_P^*(m_{K\pi})] + \tilde{\zeta}_{S4}^{\text{im}} \mathcal{R}e[\mathcal{L}_S(m_{K\pi})\mathcal{B}\mathcal{W}_P^*(m_{K\pi})] \right) \\
&+ \left. \frac{1}{2} \sin \theta_K \sin 2\theta_\ell \sin \phi \left(\tilde{\zeta}_{S5}^{\text{re}} \mathcal{I}m[\mathcal{L}_S(m_{K\pi})\mathcal{B}\mathcal{W}_P^*(m_{K\pi})] + \tilde{\zeta}_{S5}^{\text{im}} \mathcal{R}e[\mathcal{L}_S(m_{K\pi})\mathcal{B}\mathcal{W}_P^*(m_{K\pi})] \right) \right], \quad (2)
\end{aligned}$$

where $\zeta_i \equiv S_i \mp A_i$ for B^0 (\bar{B}^0) decays. The functions $\mathcal{B}\mathcal{W}_P(m_{K\pi})$ and $\mathcal{L}_S(m_{K\pi})$ describe the $m(K^+ \pi^-) \equiv m_{K\pi}$ dependence of the P- and S-wave amplitudes, respectively. The observables ζ_i are normalised by the P-wave rate, whilst those labelled $\tilde{\zeta}_i$ are normalised by the sum of P- and S-wave rates. The relative S-wave fraction is denoted as $\hat{F}_S = \frac{\Gamma_S + \bar{\Gamma}_S}{\Gamma_P + \bar{\Gamma}_P + \Gamma_S + \bar{\Gamma}_S} = 2\tilde{S}_{1a}^c - \frac{2}{3}\tilde{S}_{2a}^c$. The observable F_S is defined as $\tilde{S}_{2a}^c \equiv -\frac{3}{8}F_S$, such that in the massless lepton limit one finds $\hat{F}_S = F_S$. The coefficient S_6^s is related to the forward-backward asymmetry through $S_6^s = \frac{4}{3}A_{\text{FB}} - \frac{1}{2}S_6^c$, as discussed in Ref. [54].

Due to the choice of measuring rate-normalised observables, one of the S_i terms must be removed from the fit via

$$1 = \frac{3}{4}(2S_1^s + S_1^c) - \frac{1}{4}(2S_2^s + S_2^c). \quad (3)$$

The following additional relations between observables are used to simplify fitting models:

$$S_6^c = 0, \quad A_6^c = 0; \quad (\text{R.1})$$

$$S_1^s = 3S_2^s, \quad A_1^s = 3A_2^s; \quad (\text{R.2})$$

$$\tilde{S}_{2a}^c = -\tilde{S}_{1a}^c, \quad \tilde{A}_{1a}^c = -\tilde{A}_{2a}^c, \quad \tilde{S}_{2b}^{c,\text{re/im}} = -\tilde{S}_{1b}^{c,\text{re/im}}, \quad \tilde{A}_{2b}^{c,\text{re/im}} = -\tilde{A}_{1b}^{c,\text{re/im}}; \quad (\text{R.3})$$

$$S_1^c = -S_2^c, \quad A_1^c = -A_2^c. \quad (\text{R.4})$$

Equation R.1 holds if there are no scalar or tensor amplitudes and additionally R.2-R.4 hold if the ratio $\frac{4m_\mu^2}{q^2}$ is zero and there are no tensor amplitudes. The massless model (configurations (iv) and (v)) assumes all the relations R.1-R.4, the partially massive model (configurations (i), (ii) and (vi)) assumes relations R.1-R.3, and the fully massive model (configuration (iii)) assumes none of these relations. Pseudoexperiment studies show the relation R.4 causes larger biases on the angular observables than R.2. This is likely due to the dependence of S_1^c on the time-like amplitude. Dropping the assumption R.4, as is done for the partially massive model, reduces this bias to negligible levels for q^2 values above $\sim 1 \text{ GeV}^2/c^4$, below which the fully massive model is used. In other q^2 regions, using the fully massive model results in a loss of sensitivity significantly larger than the small bias introduced when using the partially massive model.

References

- [1] LHCb collaboration, R. Aaij *et al.*, *Angular analysis of the $B^0 \rightarrow K^{*0} \mu^+ \mu^-$ decay using 3 fb^{-1} of integrated luminosity*, JHEP **02** (2016) 104, arXiv:1512.04442.
- [2] LHCb collaboration, R. Aaij *et al.*, *Measurements of the S-wave fraction in $B^0 \rightarrow K^+ \pi^- \mu^+ \mu^-$ decays and the $B^0 \rightarrow K^*(892)^0 \mu^+ \mu^-$ differential branching fraction*, JHEP **11** (2016) 047, Erratum *ibid.* **04** (2017) 142, arXiv:1606.04731.
- [3] Belle collaboration, S. Wehle *et al.*, *Lepton-flavor-dependent angular analysis of $B \rightarrow K^* \ell^+ \ell^-$* , Phys. Rev. Lett. **118** (2017) 111801, arXiv:1612.05014.
- [4] ATLAS collaboration, M. Aaboud *et al.*, *Angular analysis of $B_d^0 \rightarrow K^* \mu^+ \mu^-$ decays in pp collisions at $\sqrt{s} = 8 \text{ TeV}$ with the ATLAS detector*, JHEP **10** (2018) 047, arXiv:1805.04000.
- [5] LHCb collaboration, R. Aaij *et al.*, *Measurement of CP-averaged observables in the $B^0 \rightarrow K^{*0} \mu^+ \mu^-$ decay*, Phys. Rev. Lett. **125** (2020) 011802, arXiv:2003.04831.
- [6] CMS collaboration, A. Hayrapetyan *et al.*, *Angular analysis of the $B^0 \rightarrow K^*(892)^0 \mu^+ \mu^-$ decay in proton-proton collisions at $\sqrt{s} = 13 \text{ TeV}$* , Phys. Lett. **B864** (2025) 139406, arXiv:2411.11820.
- [7] LHCb collaboration, R. Aaij *et al.*, *Differential branching fractions and isospin asymmetries of $B \rightarrow K^{(*)} \mu^+ \mu^-$ decays*, JHEP **06** (2014) 133, arXiv:1403.8044.
- [8] LHCb collaboration, R. Aaij *et al.*, *Angular analysis of the $B^+ \rightarrow K^{*+} \mu^+ \mu^-$ decay*, Phys. Rev. Lett. **126** (2021) 161802, arXiv:2012.13241.
- [9] LHCb collaboration, R. Aaij *et al.*, *Branching fraction measurements of the rare $B_s^0 \rightarrow \phi \mu^+ \mu^-$ and $B_s^0 \rightarrow f_2'(1525) \mu^+ \mu^-$ decays*, Phys. Rev. Lett. **127** (2021) 151801, arXiv:2105.14007.
- [10] LHCb collaboration, R. Aaij *et al.*, *Angular analysis of the rare decay $B_s^0 \rightarrow \phi \mu^+ \mu^-$* , JHEP **11** (2021) 043, arXiv:2107.13428.
- [11] S. Descotes-Genon, J. Matias, and J. Virto, *Understanding the $B \rightarrow K^* \mu^+ \mu^-$ anomaly*, Phys. Rev. **D88** (2013) 074002, arXiv:1307.5683.
- [12] F. Beaujean, C. Bobeth, and D. van Dyk, *Comprehensive Bayesian analysis of rare (semi)leptonic and radiative B decays*, Eur. Phys. J. **C74** (2014) 2897, Erratum *ibid.* **74** (2014) 3179, arXiv:1310.2478.
- [13] W. Altmannshofer and D. M. Straub, *New physics in $b \rightarrow s$ transitions after LHC run 1*, Eur. Phys. J. **C75** (2015) 382, arXiv:1411.3161.
- [14] B. Capdevila *et al.*, *Patterns of New Physics in $b \rightarrow s \ell^+ \ell^-$ transitions in the light of recent data*, JHEP **01** (2018) 093, arXiv:1704.05340.
- [15] D. London and J. Matias, *B flavour anomalies: 2021 theoretical status report*, Ann. Rev. Nucl. Part. Sci. **72** (2022) 37, arXiv:2110.13270.

- [16] N. Gubernari, M. Rebound, D. van Dyk, and J. Virto, *Improved theory predictions and global analysis of exclusive $b \rightarrow s\mu^+\mu^-$ processes*, JHEP **09** (2022) 133, [arXiv:2206.03797](#).
- [17] A. Greljo, J. Salko, A. Smolkovič, and P. Stangl, *Rare b decays meet high-mass Drell-Yan*, JHEP **05** (2023) 087, [arXiv:2212.10497](#).
- [18] M. Ciuchini *et al.*, *Constraints on lepton universality violation from rare B decays*, Phys. Rev. **D107** (2023) 055036, [arXiv:2212.10516](#).
- [19] M. Algueró *et al.*, *To $(b)e$ or not to $(b)e$: no electrons at LHCb*, Eur. Phys. J. **C83** (2023) 648, [arXiv:2304.07330](#).
- [20] A. Khodjamirian, T. Mannel, A. A. Pivovarov, and Y.-M. Wang, *Charm-loop effect in $B \rightarrow K^{(*)}\ell^+\ell^-$ and $B \rightarrow K^*\gamma$* , JHEP **09** (2010) 089, [arXiv:1006.4945](#).
- [21] A. Khodjamirian, T. Mannel, and Y.-M. Wang, *$B \rightarrow K\ell^+\ell^-$ decay at large hadronic recoil*, JHEP **02** (2013) 010, [arXiv:1211.0234](#).
- [22] HPQCD collaboration, C. Bouchard *et al.*, *Rare decay $B \rightarrow K\ell^+\ell^-$ form factors from lattice QCD*, Phys. Rev. **D88** (2013) 054509, Erratum *ibid.* **D88** (2013) 079901, [arXiv:1306.2384](#).
- [23] R. R. Horgan, Z. Liu, S. Meinel, and M. Wingate, *Lattice QCD calculation of form factors describing the rare decays $B \rightarrow K^*\ell^+\ell^-$ and $B_s \rightarrow \phi\ell^+\ell^-$* , Phys. Rev. **D89** (2014) 094501, [arXiv:1310.3722](#).
- [24] J. Lyon and R. Zwicky, *Resonances gone topsy turvy - the charm of QCD or new physics in $b \rightarrow s\ell^+\ell^-$?*, [arXiv:1406.0566](#).
- [25] R. R. Horgan, Z. Liu, S. Meinel, and M. Wingate, *Rare B decays using lattice QCD form factors*, PoS **LATTICE2014** (2015) 372, [arXiv:1501.00367](#).
- [26] J. A. Bailey *et al.*, *$B \rightarrow K\ell^+\ell^-$ decay form factors from three-flavor lattice QCD*, Phys. Rev. **D93** (2016) 025026, [arXiv:1509.06235](#).
- [27] A. Bharucha, D. M. Straub, and R. Zwicky, *$B \rightarrow V\ell^+\ell^-$ in the Standard Model from light-cone sum rules*, JHEP **08** (2016) 098, [arXiv:1503.05534](#).
- [28] A. Agadjanov, V. Bernard, U.-G. Meißner, and A. Rusetsky, *The $B \rightarrow K^*$ form factors on the lattice*, Nucl. Phys. **B910** (2016) 387, [arXiv:1605.03386](#).
- [29] A. Khodjamirian and A. V. Rusov, *$B_s \rightarrow K\ell\nu_\ell$ and $B_{(s)} \rightarrow \pi(K)\ell^+\ell^-$ decays at large recoil and CKM matrix elements*, JHEP **08** (2017) 112, [arXiv:1703.04765](#).
- [30] C. Bobeth, M. Chrzaszcz, D. van Dyk, and J. Virto, *Long-distance effects in $B \rightarrow K^*\ell\ell$ from analyticity*, Eur. Phys. J. **C78** (2018) 451, [arXiv:1707.07305](#).
- [31] N. Gubernari, A. Kokulu, and D. van Dyk, *$B \rightarrow P$ and $B \rightarrow V$ form factors from B -meson light-cone sum rules beyond leading twist*, JHEP **01** (2019) 150, [arXiv:1811.00983](#).

- [32] S. Descotes-Genon, A. Khodjamirian, and J. Virto, *Light-cone sum rules for $B \rightarrow K\pi$ form factors and applications to rare decays*, JHEP **12** (2019) 083, arXiv:1908.02267.
- [33] J. Gao *et al.*, *Precision calculations of $B \rightarrow V$ form factors from soft-collinear effective theory sum rules on the light-cone*, Phys. Rev. **D101** (2020) 074035, arXiv:1907.11092.
- [34] N. Gubernari, D. van Dyk, and J. Virto, *Non-local matrix elements in $B_{(s)} \rightarrow \{K^{(*)}, \phi\} \ell^+ \ell^-$* , JHEP **02** (2021) 088, arXiv:2011.09813.
- [35] N. Gubernari, M. Reboud, D. van Dyk, and J. Virto, *Dispersive analysis of $B \rightarrow K^{(*)}$ and $B_s \rightarrow \phi$ form factors*, JHEP **12** (2023) 153, Erratum *ibid.* **01** (2025) 125, arXiv:2305.06301.
- [36] S. Descotes-Genon, A. Khodjamirian, J. Virto, and K. K. Vos, *Light-cone sum rules for S -wave $B \rightarrow K\pi$ form factors*, JHEP **06** (2023) 034, arXiv:2304.02973.
- [37] HPQCD collaboration, W. G. Parrott, C. Bouchard, and C. T. H. Davies, *Standard Model predictions for $B \rightarrow K\ell^+\ell^-$, $B \rightarrow K\ell_1^-\ell_2^+$ and $B \rightarrow K\nu\bar{\nu}$ using form factors from $N_f = 2+1+1$ lattice QCD*, Phys. Rev. **D107** (2023) 014511, arXiv:2207.13371.
- [38] A. Y. Korchin and V. A. Kovalchuk, *Contribution of vector resonances to the $\bar{B}_d^0 \rightarrow \bar{K}^{*0}\mu^+\mu^-$ decay*, Eur. Phys. J. **C72** (2012) 2155, arXiv:1205.3683.
- [39] S. Jäger and J. Martin Camalich, *On $B \rightarrow V\ell\ell$ at small dilepton invariant mass, power corrections, and new physics*, JHEP **05** (2013) 043, arXiv:1212.2263.
- [40] S. Jäger and J. Martin Camalich, *Reassessing the discovery potential of the $B \rightarrow K^*\ell^+\ell^-$ decays in the large-recoil region: SM challenges and BSM opportunities*, Phys. Rev. **D93** (2016) 014028, arXiv:1412.3183.
- [41] M. Ciuchini *et al.*, *$B \rightarrow K^*\ell^+\ell^-$ decays at large recoil in the Standard Model: a theoretical reappraisal*, JHEP **06** (2016) 116, arXiv:1512.07157.
- [42] G. Isidori, Z. Polonsky, and A. Tinari, *Explicit estimate of charm rescattering in $B^0 \rightarrow K^0\bar{\ell}\ell$* , Phys. Rev. **D111** (2025) 093007, arXiv:2405.17551.
- [43] G. Isidori, Z. Polonsky, and A. Tinari, *Charm rescattering in $B^0 \rightarrow K^0\bar{\ell}\ell$: an improved analysis*, Eur. Phys. J. **C85** (2025) 1221, arXiv:2507.17824.
- [44] LHCb collaboration, R. Aaij *et al.*, *Amplitude analysis of the $B^0 \rightarrow K^{*0}\mu^+\mu^-$ decay*, Phys. Rev. Lett. **132** (2024) 131801, arXiv:2312.09115.
- [45] LHCb collaboration, R. Aaij *et al.*, *Comprehensive analysis of local and nonlocal amplitudes in the $B^0 \rightarrow K^{*0}\mu^+\mu^-$ decay*, JHEP **09** (2024) 026, Erratum *ibid.* **05** (2025) 208, arXiv:2405.17347.
- [46] LHCb collaboration, R. Aaij *et al.*, *Differential branching fraction and angular analysis of the decay $B^0 \rightarrow K^{*0}\mu^+\mu^-$* , Phys. Rev. Lett. **108** (2012) 181806, arXiv:1112.3515.
- [47] LHCb collaboration, R. Aaij *et al.*, *Differential branching fraction and angular analysis of the decay $B^0 \rightarrow K^{*0}\mu^+\mu^-$* , JHEP **08** (2013) 131, arXiv:1304.6325.

- [48] LHCb collaboration, R. Aaij *et al.*, *Measurement of form-factor-independent observables in the decay $B^0 \rightarrow K^{*0} \mu^+ \mu^-$* , Phys. Rev. Lett. **111** (2013) 191801, arXiv:1308.1707.
- [49] LHCb collaboration, R. Aaij *et al.*, *Measurement of CP asymmetries in the decays $B^0 \rightarrow K^{*0} \mu^+ \mu^-$ and $B^+ \rightarrow K^+ \mu^+ \mu^-$* , JHEP **09** (2014) 177, arXiv:1408.0978.
- [50] M. Algueró *et al.*, *A complete description of P- and S-wave contributions to the $B^0 \rightarrow K^+ \pi^- \ell^+ \ell^-$ decay*, JHEP **12** (2021) 085, arXiv:2107.05301.
- [51] A. Ali, P. Ball, L. T. Handoko, and G. Hiller, *A comparative study of the decays $B \rightarrow (K, K^*) \ell^+ \ell^-$ in standard model and supersymmetric theories*, Phys. Rev. **D61** (2000) 074024, arXiv:hep-ph/9910221.
- [52] F. Krüger, L. M. Sehgal, N. Sinha, and R. Sinha, *Angular distribution and CP asymmetries in the decays $\bar{B} \rightarrow K^- \pi^+ e^- e^+$ and $\bar{B} \rightarrow \pi^- \pi^+ e^- e^+$* , Phys. Rev. **D61** (2000) 114028, Erratum *ibid.* **D63** (2000) 019901, arXiv:hep-ph/9907386.
- [53] F. Krüger and J. Matias, *Probing new physics via the transverse amplitudes of $B^0 \rightarrow K^{*0} (\rightarrow K^- \pi^+) \ell^+ \ell^-$ at large recoil*, Phys. Rev. **D71** (2005) 094009, arXiv:hep-ph/0502060.
- [54] W. Altmannshofer *et al.*, *Symmetries and asymmetries of $B \rightarrow K^* \mu^+ \mu^-$ decays in the Standard Model and beyond*, JHEP **01** (2009) 019, arXiv:0811.1214.
- [55] U. Egede *et al.*, *New observables in the decay mode $\bar{B}_d \rightarrow \bar{K}^{*0} \ell^+ \ell^-$* , JHEP **11** (2008) 032, arXiv:0807.2589.
- [56] D. Bečirević and E. Schneider, *On transverse asymmetries in $B \rightarrow K^* \ell^+ \ell^-$* , Nucl. Phys. **B854** (2012) 321, arXiv:1106.3283.
- [57] C. Bobeth, G. Hiller, and D. van Dyk, *The benefits of $\bar{B} \rightarrow \bar{K}^* \ell^+ \ell^-$ decays at low recoil*, JHEP **07** (2010) 098, arXiv:1006.5013.
- [58] U. Egede *et al.*, *On the new physics reach of the decay mode $\bar{B}_d \rightarrow \bar{K}^{*0} \ell^+ \ell^-$* , JHEP **10** (2010) 056, arXiv:1005.0571.
- [59] C. Bobeth, G. Hiller, and D. van Dyk, *More benefits of semileptonic rare B decays at low recoil: CP violation*, JHEP **07** (2011) 067, arXiv:1105.0376.
- [60] C. Bobeth, G. Hiller, and D. van Dyk, *General analysis of $\bar{B} \rightarrow \bar{K}^{(*)} \ell^+ \ell^-$ decays at low recoil*, Phys. Rev. **D87** (2013) 034016, arXiv:1212.2321.
- [61] J. Matias, F. Mescia, M. Ramon, and J. Virto, *Complete anatomy of $\bar{B}_d \rightarrow \bar{K}^{*0} (\rightarrow K \pi) \ell^+ \ell^-$ and its angular distribution*, JHEP **04** (2012) 104, arXiv:1202.4266.
- [62] J. Matias, *On the S-wave pollution of $B \rightarrow K^* \ell^+ \ell^-$ observables*, Phys. Rev. **D86** (2012) 094024, arXiv:1209.1525.
- [63] C. Bobeth, G. Hiller, and G. Piranishvili, *CP asymmetries in $\bar{B} \rightarrow \bar{K}^* (\rightarrow \bar{K} \pi) \bar{\ell} \ell$ and untagged $\bar{B}_s, B_s \rightarrow \phi (\rightarrow K^+ K^-) \bar{\ell} \ell$ decays at NLO*, JHEP **07** (2008) 106, arXiv:0805.2525.

- [64] S. Descotes-Genon, J. Matias, M. Ramon, and J. Virto, *Implications from clean observables for the binned analysis of $B \rightarrow K^* \mu^+ \mu^-$ at large recoil*, JHEP **01** (2013) 048, [arXiv:1207.2753](#).
- [65] G. Kumar and N. Mahajan, *$B \rightarrow K^* \ell^+ \ell^-$: Zeroes of angular observables as test of standard model*, Phys. Rev. **D93** (2016) 054041, [arXiv:1412.2955](#).
- [66] LHCb collaboration, A. A. Alves Jr. *et al.*, *The LHCb detector at the LHC*, JINST **3** (2008) S08005.
- [67] LHCb collaboration, R. Aaij *et al.*, *LHCb detector performance*, Int. J. Mod. Phys. **A30** (2015) 1530022, [arXiv:1412.6352](#).
- [68] R. Aaij *et al.*, *The LHCb trigger and its performance in 2011*, JINST **8** (2013) P04022, [arXiv:1211.3055](#).
- [69] N. Grieser *et al.*, *The LHCb stripping project: Sustainable legacy data processing for high-energy physics*, Comput. Softw. Big. Sci. **9** (2025) 21, [arXiv:2509.05294](#).
- [70] T. Sjöstrand, S. Mrenna, and P. Skands, *A brief introduction to PYTHIA 8.1*, Comput. Phys. Commun. **178** (2008) 852, [arXiv:0710.3820](#).
- [71] D. J. Lange, *The EvtGen particle decay simulation package*, Nucl. Instrum. Meth. **A462** (2001) 152.
- [72] Geant4 collaboration, J. Allison *et al.*, *Geant4 developments and applications*, IEEE Trans. Nucl. Sci. **53** (2006) 270; Geant4 collaboration, S. Agostinelli *et al.*, *Geant4: A simulation toolkit*, Nucl. Instrum. Meth. **A506** (2003) 250.
- [73] L. Anderlini *et al.*, *The PIDCalib package*, LHCb-PUB-2016-021, 2016.
- [74] R. Aaij *et al.*, *Selection and processing of calibration samples to measure the particle identification performance of the LHCb experiment in Run 2*, Eur. Phys. J. Tech. Instr. **6** (2019) 1, [arXiv:1803.00824](#).
- [75] LHCb collaboration, R. Aaij *et al.*, *Measurement of the track reconstruction efficiency at LHCb*, JINST **10** (2015) P02007, [arXiv:1408.1251](#).
- [76] L. Breiman, J. H. Friedman, R. A. Olshen, and C. J. Stone, *Classification and regression trees*, Wadsworth international group, Belmont, California, USA, 1984.
- [77] Y. Freund and R. E. Schapire, *A decision-theoretic generalization of on-line learning and an application to boosting*, J. Comput. Syst. Sci. **55** (1997) 119.
- [78] M. Pivk and F. R. Le Diberder, *sPlot: A statistical tool to unfold data distributions*, Nucl. Instrum. Meth. **A555** (2005) 356, [arXiv:physics/0402083](#).
- [79] A. Blum, A. T. Kalai, and J. Langford, *Beating the hold-out: bounds for k-fold and progressive cross-validation*, in *Annual Conference Computational Learning Theory*, 1999.
- [80] LHCb collaboration, R. Aaij *et al.*, *Search for the rare decays $B_s^0 \rightarrow \mu^+ \mu^-$ and $B^0 \rightarrow \mu^+ \mu^-$* , Phys. Lett. **B699** (2011) 330, [arXiv:1103.2465](#).

- [81] Particle Data Group, S. Navas *et al.*, *Review of particle physics*, Phys. Rev. **D110** (2024) 030001.
- [82] C. Weisser and M. Williams, *Machine learning and multivariate goodness of fit*, arXiv:1612.07186.
- [83] Belle collaboration, K. Chilikin *et al.*, *Observation of a new charged charmoniumlike state in $\bar{B}^0 \rightarrow J/\psi K^- \pi^+$ decays*, Phys. Rev. **D90** (2014) 112009, arXiv:1408.6457.
- [84] LHCb collaboration, R. Aaij *et al.*, *Measurement of the polarization amplitudes in $B^0 \rightarrow J/\psi K^*(892)^0$ decays*, Phys. Rev. **D88** (2013) 052002, arXiv:1307.2782.
- [85] J. M. Blatt and V. F. Weisskopf, *Theoretical nuclear physics*, Springer, New York, 1952.
- [86] D. Aston *et al.*, *A study of $K^- \pi^+$ scattering in the reaction $K^- p \rightarrow K^- \pi^+ n$ at 11 GeV/c*, Nucl. Phys. **B296** (1988) 493.
- [87] Z. Rui and W.-F. Wang, *S-wave $K\pi$ contributions to the hadronic charmonium B decays in the perturbative QCD approach*, Phys. Rev. **D97** (2018) 033006, arXiv:1711.08959.
- [88] LHCb collaboration, R. Aaij *et al.*, *Observation of the resonant character of the $Z(4430)^-$ state*, Phys. Rev. Lett. **112** (2014) 222002, arXiv:1404.1903.
- [89] Belle collaboration, K. Chilikin *et al.*, *Experimental constraints on the spin and parity of the $Z(4430)^+$* , Phys. Rev. **D88** (2013) 074026, arXiv:1306.4894.
- [90] T. Skwarnicki, *A study of the radiative cascade transitions between the Upsilon-prime and Upsilon resonances*, PhD thesis, Institute of Nuclear Physics, Krakow, 1986, DESY-F31-86-02.
- [91] J. Neyman, *Outline of a theory of statistical estimation based on the classical theory of probability*, Phil. Trans. Roy. Soc. Lond. **A236** (1937) 333.
- [92] M. Williams, *How good are your fits? Unbinned multivariate goodness-of-fit tests in high energy physics*, JINST **5** (2010) P09004, arXiv:1006.3019.
- [93] D. M. Straub, *flavio: a Python package for flavour and precision phenomenology in the Standard Model and beyond*, arXiv:1810.08132.
- [94] EOS Authors collaboration, D. van Dyk *et al.*, *EOS: a software for flavor physics phenomenology*, Eur. Phys. J. **C82** (2022) 569, arXiv:2111.15428.
- [95] N. Gubernari, M. Reboud, D. van Dyk, and J. Virto, *Improved theory predictions and global analysis of exclusive $b \rightarrow s\mu^+\mu^-$ processes*, JHEP **09** (2022) 133, arXiv:2206.03797.

LHCb collaboration

R. Aaij³⁸ , A.S.W. Abdelmotteleb⁵⁸ , C. Abellan Beteta⁵² , F. Abudinén⁵⁸ ,
T. Ackernley⁶² , A. A. Adefisoye⁷⁰ , B. Adeva⁴⁸ , M. Adinolfi⁵⁶ , P. Adlarson⁸⁶ ,
C. Agapopoulou¹⁴ , C.A. Aidala⁸⁸ , Z. Ajaltouni¹¹, S. Akar¹¹ , K. Akiba³⁸ , M.
Akthar⁴⁰ , P. Albicocco²⁸ , J. Albrecht^{19,g} , R. Aleksiejunas⁸² , F. Alessio⁵⁰ ,
P. Alvarez Cartelle⁵⁷ , R. Amalric¹⁶ , S. Amato³ , J.L. Amey⁵⁶ , Y. Amhis¹⁴ ,
L. An⁶ , L. Anderlini²⁷ , M. Andersson⁵² , P. Andreola⁵² , M. Andreotti²⁶ , S.
Andres Estrada⁴⁵ , A. Anelli^{31,p,50} , D. Ao⁷ , C. Arata¹² , F. Archilli^{37,w} , Z. Areg⁷⁰ ,
M. Argenton²⁶ , S. Arguedas Cuendis^{9,50} , L. Arnone^{31,p} , A. Artamonov⁴⁴ ,
M. Artuso⁷⁰ , E. Aslanides¹³ , R. Ataíde Da Silva⁵¹ , M. Atzeni⁶⁶ , B. Audurier¹² , J.
A. Authier¹⁵ , D. Bacher⁶⁵ , I. Bachiller Perea⁵¹ , S. Bachmann²² , M. Bachmayer⁵¹ ,
J.J. Back⁵⁸ , P. Baladron Rodriguez⁴⁸ , V. Balagura¹⁵ , A. Balboni²⁶ , W. Baldini²⁶ ,
Z. Baldwin⁸⁰ , L. Balzani¹⁹ , H. Bao⁷ , J. Baptista de Souza Leite² ,
C. Barbero Pretel^{48,12} , M. Barbetti²⁷ , I. R. Barbosa⁷¹ , R.J. Barlow⁶⁴ ,
M. Barnyakov²⁵ , S. Barsuk¹⁴ , W. Barter⁶⁰ , J. Bartz⁷⁰ , S. Bashir⁴⁰ , B. Batsukh⁵ ,
P. B. Battista¹⁴ , A. Bay⁵¹ , A. Beck⁶⁶ , M. Becker¹⁹ , F. Bedeschi³⁵ , I.B. Bediaga² ,
N. A. Behling¹⁹ , S. Belin⁴⁸ , A. Bellavista²⁵ , K. Belous⁴⁴ , I. Belov²⁹ ,
I. Belyaev³⁶ , G. Benane¹³ , G. Bencivenni²⁸ , E. Ben-Haim¹⁶ , A. Berezhnoy⁴⁴ ,
R. Bernet⁵² , S. Bernet Andres⁴⁷ , A. Bertolin³³ , F. Betti⁶⁰ , J. Bex⁵⁷ ,
O. Bezshyyko⁸⁷ , S. Bhattacharya⁸¹ , J. Bhom⁴¹ , M.S. Bieker¹⁸ , N.V. Biesuz²⁶ ,
A. Biolchini³⁸ , M. Birch⁶³ , F.C.R. Bishop¹⁰ , A. Bitadze⁶⁴ , A. Bizzetti^{27,q} ,
T. Blake^{58,c} , F. Blanc⁵¹ , J.E. Blank¹⁹ , S. Blusk⁷⁰ , V. Bocharnikov⁴⁴ ,
J.A. Boelhauve¹⁹ , O. Boente Garcia⁵⁰ , T. Boettcher⁶⁹ , A. Bohare⁶⁰ , A. Boldyrev⁴⁴ ,
C. Bolognani⁸⁴ , R. Bolzonella^{26,m} , R. B. Bonacci¹ , N. Bondar^{44,50} , A. Bordelius⁵⁰ ,
F. Borgato^{33,50} , S. Borghi⁶⁴ , M. Borsato^{31,p} , J.T. Borsuk⁸⁵ , E. Botalico⁶² ,
S.A. Bouchiba⁵¹ , M. Bovill⁶⁵ , T.J.V. Bowcock⁶² , A. Boyer⁵⁰ , C. Bozzi²⁶ , J.
D. Brandenburg⁸⁹ , A. Brea Rodriguez⁵¹ , N. Breer¹⁹ , J. Brodzicka⁴¹ , J. Brown⁶² ,
D. Brundu³² , E. Buchanan⁶⁰ , M. Burgos Marcos⁸⁴ , A.T. Burke⁶⁴ , C. Burr⁵⁰ , C.
Buti²⁷ , J.S. Butter⁵⁷ , J. Buytaert⁵⁰ , W. Byczynski⁵⁰ , S. Cadeddu³² , H. Cai⁷⁶ , Y.
Cai⁵ , A. Caillet¹⁶ , R. Calabrese^{26,m} , S. Calderon Ramirez⁹ , L. Calefice⁴⁶ ,
M. Calvi^{31,p} , M. Calvo Gomez⁴⁷ , P. Camargo Magalhaes^{2,a} , J. I. Cambon Bouzas⁴⁸ ,
P. Campana²⁸ , A.F. Campoverde Quezada⁷ , S. Capelli³¹ , M. Caporale²⁵ ,
L. Capriotti²⁶ , R. Caravaca-Mora⁹ , A. Carbone^{25,k} , L. Carcedo Salgado⁴⁸ ,
R. Cardinale^{29,n} , A. Cardini³² , P. Carniti³¹ , L. Carus²² , A. Casais Vidal⁶⁶ ,
R. Caspary²² , G. Casse⁶² , M. Cattaneo⁵⁰ , G. Cavallero²⁶ , V. Cavallini^{26,m} ,
S. Celani⁵⁰ , I. Celestino^{35,t} , S. Cesare^{30,o} , A.J. Chadwick⁶² , I. Chahrouh⁸⁸ , H.
Chang^{4,d} , M. Charles¹⁶ , Ph. Charpentier⁵⁰ , E. Chatzianagnostou³⁸ , R. Cheaib⁸¹ ,
M. Chefdeville¹⁰ , C. Chen⁵⁷ , J. Chen⁵¹ , S. Chen⁵ , Z. Chen⁷ , A. Chen Hu⁶³ , M.
Cherif¹² , A. Chernov⁴¹ , S. Chernyshenko⁵⁴ , X. Chiotopoulos⁸⁴ , V. Chobanova⁴⁵ ,
M. Chrzaszcz⁴¹ , A. Chubykin⁴⁴ , V. Chulikov^{28,36,50} , P. Ciambone²⁸ ,
X. Cid Vidal⁴⁸ , G. Ciezarek⁵⁰ , P. Cifra³⁸ , P.E.L. Clarke⁶⁰ , M. Clemencic⁵⁰ ,
H.V. Cliff⁵⁷ , J. Closier⁵⁰ , C. Cocha Toapaxi²² , V. Coco⁵⁰ , J. Cogan¹³ ,
E. Cogneras¹¹ , L. Cojocariu⁴³ , S. Collaviti⁵¹ , P. Collins⁵⁰ , T. Colombo⁵⁰ ,
M. Colonna¹⁹ , A. Comerma-Montells⁴⁶ , L. Congedo²⁴ , J. Connaughton⁵⁸ ,
A. Contu³² , N. Cooke⁶¹ , G. Cordova^{35,t} , C. Coronel⁶⁷ , I. Corredoira¹² ,
A. Correia¹⁶ , G. Corti⁵⁰ , J. Cottee Meldrum⁵⁶ , B. Couturier⁵⁰ , D.C. Craik⁵² ,
M. Cruz Torres^{2,h} , E. Curras Rivera⁵¹ , R. Currie⁶⁰ , C.L. Da Silva⁶⁹ ,
S. Dadabaev⁴⁴ , X. Dai⁴ , E. Dall'Occo⁵⁰ , J. Dalseno⁴⁵ , C. D'Ambrosio⁶³ ,
J. Daniel¹¹ , G. Darze³ , A. Davidson⁵⁸ , J.E. Davies⁶⁴ , O. De Aguiar Francisco⁶⁴ ,

C. De Angelis^{32,l} , F. De Benedetti⁵⁰ , J. de Boer³⁸ , K. De Bruyn⁸³ , S. De Capua⁶⁴ ,
 M. De Cian^{64,50} , U. De Freitas Carneiro Da Graca^{2,b} , E. De Lucia²⁸ ,
 J.M. De Miranda² , L. De Paula³ , M. De Serio^{24,i} , P. De Simone²⁸ , F. De Vellis¹⁹ ,
 J.A. de Vries⁸⁴ , F. Debernardis²⁴ , D. Decamp¹⁰ , S. Dekkers¹ , L. Del Buono¹⁶ ,
 B. Delaney⁶⁶ , H.-P. Dembinski¹⁹ , J. Deng⁸ , V. Denysenko⁵² , O. Deschamps¹¹ ,
 F. Dettori^{32,l} , B. Dey⁸¹ , P. Di Nezza²⁸ , I. Diachkov⁴⁴ , S. Didenko⁴⁴ , S. Ding⁷⁰ ,
 Y. Ding⁵¹ , L. Dittmann²² , V. Dobishuk⁵⁴ , A. D. Docheva⁶¹ , A. Doheny⁵⁸ ,
 C. Dong^{4,d} , A.M. Donohoe²³ , F. Dordei³² , A.C. dos Reis² , A. D. Dowling⁷⁰ ,
 L. Dreyfus¹³ , W. Duan⁷⁴ , P. Duda⁸⁵ , L. Dufour⁵⁰ , V. Duk³⁴ , P. Durante⁵⁰ , M.
 M. Duras⁸⁵ , J.M. Durham⁶⁹ , O. D. Durmus⁸¹ , A. Dziurda⁴¹ , A. Dzyuba⁴⁴ ,
 S. Easo⁵⁹ , E. Eckstein¹⁸ , U. Egede¹ , A. Egorychev⁴⁴ , V. Egorychev⁴⁴ ,
 S. Eisenhardt⁶⁰ , E. Ejopu⁶² , L. Eklund⁸⁶ , M. Elashri⁶⁷ , D. Elizondo Blanco⁹ ,
 J. Ellbracht¹⁹ , S. Ely⁶³ , A. Ene⁴³ , J. Eschle⁷⁰ , S. Esen²² , T. Evans³⁸ ,
 F. Fabiano³² , S. Faghih⁶⁷ , L.N. Falcao² , B. Fang⁷ , R. Fantechi³⁵ , L. Fantini^{34,s} ,
 M. Faria⁵¹ , K. Farmer⁶⁰ , F. Fassin^{83,38} , D. Fazzini^{31,p} , L. Felkowski⁸⁵ ,
 M. Feng^{5,7} , A. Fernandez Casani⁴⁹ , M. Fernandez Gomez⁴⁸ , A.D. Fernez⁶⁸ ,
 F. Ferrari^{25,k} , F. Ferreira Rodrigues³ , M. Ferrillo⁵² , M. Ferro-Luzzi⁵⁰ , S. Filippov⁴⁴ ,
 R.A. Fini²⁴ , M. Fiorini^{26,m} , M. Firlej⁴⁰ , K.L. Fischer⁶⁵ , D.S. Fitzgerald⁸⁸ ,
 C. Fitzpatrick⁶⁴ , T. Fiutowski⁴⁰ , F. Fleuret¹⁵ , A. Fomin⁵³ , M. Fontana²⁵ , L. A.
 Foreman⁶⁴ , R. Forty⁵⁰ , D. Foulds-Holt⁶⁰ , V. Franco Lima³ , M. Franco Sevilla⁶⁸ ,
 M. Frank⁵⁰ , E. Franzoso^{26,m} , G. Frau⁶⁴ , C. Frei⁵⁰ , D.A. Friday^{64,50} , J. Fu⁷ ,
 Q. Führung^{19,g,57} , T. Fulghesu¹³ , G. Galati²⁴ , M.D. Galati³⁸ , A. Gallas Torreira⁴⁸ ,
 D. Galli^{25,k} , S. Gambetta⁶⁰ , M. Gandelman³ , P. Gandini³⁰ , B. Ganie⁶⁴ ,
 H. Gao⁷ , R. Gao⁶⁵ , T.Q. Gao⁵⁷ , Y. Gao⁸ , Y. Gao⁶ , Y. Gao⁸ ,
 L.M. Garcia Martin⁵¹ , P. Garcia Moreno⁴⁶ , J. García Pardiñas⁶⁶ , P. Gardner⁶⁸ ,
 L. Garrido⁴⁶ , C. Gaspar⁵⁰ , A. Gavrikov³³ , L.L. Gerken¹⁹ , E. Gersabeck²⁰ ,
 M. Gersabeck²⁰ , T. Gershon⁵⁸ , S. Ghizzo^{29,n} , Z. Ghorbanimoghaddam⁵⁶ , F.
 I. Giasemis^{16,f} , V. Gibson⁵⁷ , H.K. Gienza⁴² , A.L. Gilman⁶⁷ , M. Giovannetti²⁸ ,
 A. Gioventù⁴⁶ , L. Girardey^{64,59} , M.A. Giza⁴¹ , F.C. Glaser^{14,22} , V.V. Gligorov¹⁶ ,
 C. Göbel⁷¹ , L. Golinka-Bezshyyko⁸⁷ , E. Golobardes⁴⁷ , D. Golubkov⁴⁴ ,
 A. Golutvin^{63,50} , S. Gomez Fernandez⁴⁶ , W. Gomulka⁴⁰ , I. Gonçalves Vaz⁵⁰ ,
 F. Goncalves Abrantes⁶⁵ , M. Goncerz⁴¹ , G. Gong^{4,d} , J. A. Gooding¹⁹ ,
 I.V. Gorelov⁴⁴ , C. Gotti³¹ , E. Govorkova⁶⁶ , J.P. Grabowski³⁰ ,
 L.A. Granado Cardoso⁵⁰ , E. Graugés⁴⁶ , E. Graverini^{51,u} , L. Grazette⁵⁸ ,
 G. Graziani²⁷ , A. T. Grecu⁴³ , N.A. Grieser⁶⁷ , L. Grillo⁶¹ , S. Gromov⁴⁴ , C. Gu¹⁵ ,
 M. Guarise²⁶ , L. Guerry¹¹ , A.-K. Guseinov⁵¹ , E. Gushchin⁴⁴ , Y. Guz^{6,50} ,
 T. Gys⁵⁰ , K. Habermann¹⁸ , T. Hadavizadeh¹ , C. Hadjivasiliou⁶⁸ , G. Haefeli⁵¹ ,
 C. Haen⁵⁰ , S. Haken⁵⁷ , G. Hallett⁵⁸ , P.M. Hamilton⁶⁸ , J. Hammerich⁶² ,
 Q. Han³³ , X. Han^{22,50} , S. Hansmann-Menzemer²² , L. Hao⁷ , N. Harnew⁶⁵ , T. H.
 Harris¹ , M. Hartmann¹⁴ , S. Hashmi⁴⁰ , J. He^{7,e} , A. Hedes⁶⁴ , F. Hemmer⁵⁰ ,
 C. Henderson⁶⁷ , R. Henderson¹⁴ , R.D.L. Henderson¹ , A.M. Hennequin⁵⁰ ,
 K. Hennessy⁶² , L. Henry⁵¹ , J. Herd⁶³ , P. Herrero Gascon²² , J. Heuel¹⁷ , A.
 Heyn¹³ , A. Hicheur³ , G. Hijano Mendizabal⁵² , J. Horswill⁶⁴ , R. Hou⁸ , Y. Hou¹¹ ,
 D.C. Houston⁶¹ , N. Howarth⁶² , W. Hu⁷ , X. Hu⁴ , W. Hulsbergen³⁸ ,
 R.J. Hunter⁵⁸ , M. Hushchyn⁴⁴ , D. Hutchcroft⁶² , M. Idzik⁴⁰ , D. Ilin⁴⁴ , P. Ilten⁶⁷ ,
 A. Iniukhin⁴⁴ , A. Iohner¹⁰ , A. Ishteev⁴⁴ , K. Ivshin⁴⁴ , H. Jage¹⁷ ,
 S.J. Jaimes Elles^{78,49,50} , S. Jakobsen⁵⁰ , T. Jakoubek⁷⁹ , E. Jans³⁸ , B.K. Jashal⁴⁹ ,
 A. Jawahery⁶⁸ , C. Jayaweera⁵⁵ , V. Jevtic¹⁹ , Z. Jia¹⁶ , E. Jiang⁶⁸ , X. Jiang^{5,7} ,
 Y. Jiang⁷ , Y. J. Jiang⁶ , E. Jimenez Moya⁹ , N. Jindal⁸⁹ , M. John⁶⁵ , A.
 John Rubesh Rajan²³ , D. Johnson⁵⁵ , C.R. Jones⁵⁷ , S. Joshi⁴² , B. Jost⁵⁰ , J.

Juan Castella⁵⁷ , N. Jurik⁵⁰ , I. Juszczak⁴¹ , K. Kalecinska⁴⁰, D. Kaminaris⁵¹ ,
 S. Kandybei⁵³ , M. Kane⁶⁰ , Y. Kang^{4,d} , C. Kar¹¹ , M. Karacson⁵⁰ ,
 A. Kauniskangas⁵¹ , J.W. Kautz⁶⁷ , M.K. Kazanecki⁴¹ , F. Keizer⁵⁰ , M. Kenzie⁵⁷ ,
 T. Ketel³⁸ , B. Khanji⁷⁰ , A. Kharisova⁴⁴ , S. Kholodenko^{63,50} , G. Khreich¹⁴ ,
 T. Kirn¹⁷ , V.S. Kirsebom^{31,p} , O. Kitouni⁶⁶ , S. Klaver³⁹ , N. Kleijne^{35,t} , D. K.
 Klekots⁸⁷ , K. Klimaszewski⁴² , M.R. Kmiec⁴² , T. Knospe¹⁹ , R. Kolb²² ,
 S. Koliiev⁵⁴ , L. Kolk¹⁹ , A. Konoplyannikov⁶ , P. Kopciwicz⁵⁰ , P. Koppenburg³⁸ , A.
 Korchin⁵³ , M. Korolev⁴⁴ , I. Kostiuk³⁸ , O. Kot⁵⁴ , S. Kotriakhova , E.
 Kowalczyk⁶⁸ , A. Kozachuk⁴⁴ , P. Kravchenko⁴⁴ , L. Kravchuk⁴⁴ , O. Kravcov⁸² ,
 M. Kreps⁵⁸ , P. Krovovny⁴⁴ , W. Krupa⁷⁰ , W. Krzemien⁴² , O. Kshyvanskyi⁵⁴ ,
 S. Kubis⁸⁵ , M. Kucharczyk⁴¹ , V. Kudryavtsev⁴⁴ , E. Kulikova⁴⁴ , A. Kupsc⁸⁶ ,
 V. Kushnir⁵³ , B. Kutsenko¹³ , J. Kvapil⁶⁹ , I. Kyryllin⁵³ , D. Lacarrere⁵⁰ , P.
 Laguarda Gonzalez⁴⁶ , A. Lai³² , A. Lampis³² , D. Lancierini⁶³ , C. Landesa Gomez⁴⁸ ,
 J.J. Lane¹ , G. Lanfranchi²⁸ , C. Langenbruch²² , J. Langer¹⁹ , T. Latham⁵⁸ ,
 F. Lazzari^{35,u,50} , C. Lazzeroni⁵⁵ , R. Le Gac¹³ , H. Lee⁶² , R. Lefèvre¹¹ ,
 A. Leflat⁴⁴ , S. Legotin⁴⁴ , M. Lehuraux⁵⁸ , E. Lemos Cid⁵⁰ , O. Leroy¹³ ,
 T. Lesiak⁴¹ , E. D. Lesser⁵⁰ , B. Leverington²² , A. Li^{4,d} , C. Li^{4,d} , C. Li¹³ ,
 H. Li⁷⁴ , J. Li⁸ , K. Li⁷⁷ , L. Li⁶⁴ , M. Li⁸ , P. Li⁷ , P.-R. Li⁷⁵ , Q. Li^{5,7} ,
 T. Li⁷³ , T. Li⁷⁴ , Y. Li⁸ , Y. Li⁵ , Y. Li⁴ , Z. Lian^{4,d} , Q. Liang⁸, X. Liang⁷⁰ , Z.
 Liang³² , S. Libralon⁴⁹ , A. Lightbody¹² , C. Lin⁷ , T. Lin⁵⁹ , R. Lindner⁵⁰ , H.
 Linton⁶³ , R. Litvinov³² , D. Liu⁸ , F. L. Liu¹ , G. Liu⁷⁴ , K. Liu⁷⁵ , S. Liu⁵ , W.
 Liu⁸ , Y. Liu⁶⁰ , Y. Liu⁷⁵ , Y. L. Liu⁶³ , G. Loachamin Ordonez⁷¹ , I. Lobo¹ ,
 A. Lobo Salvia⁴⁶ , A. Loi³² , T. Long⁵⁷ , F. C. L. Lopes^{2,a} , J.H. Lopes³ ,
 A. Lopez Huertas⁴⁶ , C. Lopez Iribarnegaray⁴⁸ , S. López Soliño⁴⁸ , Q. Lu¹⁵ ,
 C. Lucarelli⁵⁰ , D. Lucchesi^{33,r} , M. Lucio Martinez⁴⁹ , Y. Luo⁶ , A. Lupato^{33,j} ,
 E. Luppi^{26,m} , K. Lynch²³ , X.-R. Lyu⁷ , G. M. Ma^{4,d} , H. Ma⁷³ , S. Maccolini¹⁹ ,
 F. Machefert¹⁴ , F. Maciuc⁴³ , B. Mack⁷⁰ , I. Mackay⁶⁵ , L. M. Mackey⁷⁰ ,
 L.R. Madhan Mohan⁵⁷ , M. J. Madurai⁵⁵ , D. Magdalinski³⁸ , D. Maisuzenko⁴⁴ ,
 J.J. Malczewski⁴¹ , S. Malde⁶⁵ , L. Malentacca⁵⁰ , A. Malinin⁴⁴ , T. Maltsev⁴⁴ ,
 G. Manca^{32,l} , G. Mancinelli¹³ , C. Mancuso¹⁴ , R. Manera Escalero⁴⁶ , F. M.
 Manganella³⁷ , D. Manuzzi²⁵ , D. Marangotto^{30,o} , J.F. Marchand¹⁰ ,
 R. Marchevski⁵¹ , U. Marconi²⁵ , E. Mariani¹⁶ , S. Mariani⁵⁰ , C. Marin Benito⁴⁶ ,
 J. Marks²² , A.M. Marshall⁵⁶ , L. Martel⁶⁵ , G. Martelli³⁴ , G. Martellotti³⁶ ,
 L. Martinazzoli⁵⁰ , M. Martinelli^{31,p} , D. Martinez Gomez⁸³ , D. Martinez Santos⁴⁵ ,
 F. Martinez Vidal⁴⁹ , A. Martorell i Granollers⁴⁷ , A. Massafferri² , R. Matev⁵⁰ ,
 A. Mathad⁵⁰ , V. Matiuin⁴⁴ , C. Matteuzzi⁷⁰ , K.R. Mattioli¹⁵ , A. Mauri⁶³ ,
 E. Maurice¹⁵ , J. Mauricio⁴⁶ , P. Mayencourt⁵¹ , J. Mazorra de Cos⁴⁹ , M. Mazurek⁴² ,
 M. McCann⁶³ , N.T. McHugh⁶¹ , A. McNab⁶⁴ , R. McNulty²³ , B. Meadows⁶⁷ ,
 G. Meier¹⁹ , D. Melnychuk⁴² , D. Mendoza Granada¹⁶ , P. Menendez Valdes Perez⁴⁸ , F.
 M. Meng^{4,d} , M. Merk^{38,84} , A. Merli^{51,30} , L. Meyer Garcia⁶⁸ , D. Miao^{5,7} ,
 H. Miao⁷ , M. Mikhasenko⁸⁰ , D.A. Milanes^{78,z} , A. Minotti^{31,p} , E. Minucci²⁸ ,
 T. Miralles¹¹ , B. Mitreska⁶⁴ , D.S. Mitzel¹⁹ , R. Mocanu⁴³ , A. Modak⁵⁹ ,
 L. Moeser¹⁹ , R.D. Moise¹⁷ , E. F. Molina Cardenas⁸⁸ , T. Mombächer⁶⁷ , M. Monk⁵⁷ ,
 S. Monteil¹¹ , A. Morcillo Gomez⁴⁸ , G. Morello²⁸ , M.J. Morello^{35,t} ,
 M.P. Morgenthaler²² , A. Moro^{31,p} , J. Moron⁴⁰ , W. Morren³⁸ , A.B. Morris⁵⁰ ,
 A.G. Morris¹³ , R. Mountain⁷⁰ , Z. M. Mu⁶ , E. Muhammad⁵⁸ , F. Muheim⁶⁰ ,
 M. Mulder⁸³ , K. Müller⁵² , F. Muñoz-Rojas⁹ , R. Murta⁶³ , V. Mytrochenko⁵³ ,
 P. Naik⁶² , T. Nakada⁵¹ , R. Nandakumar⁵⁹ , T. Nanut⁵⁰ , I. Nasteva³ ,
 M. Needham⁶⁰ , E. Nekrasova⁴⁴ , N. Neri^{30,o} , S. Neubert¹⁸ , N. Neufeld⁵⁰ ,
 P. Neustroev⁴⁴ , J. Nicolini⁵⁰ , D. Nicotra⁸⁴ , E.M. Niel¹⁵ , N. Nikitin⁴⁴ , L. Nisi¹⁹ ,

Q. Niu⁷⁵ , P. Nogarolli³ , P. Nogga¹⁸ , C. Normand⁵⁶ , J. Novoa Fernandez⁴⁸ ,
 G. Nowak⁶⁷ , C. Nunez⁸⁸ , H. N. Nur⁶¹ , A. Oblakowska-Mucha⁴⁰ , V. Obratsov⁴⁴ ,
 T. Oeser¹⁷ , A. Okhotnikov⁴⁴ , O. Okhrimenko⁵⁴ , R. Oldeman^{32,l} , F. Oliva^{60,50} , E.
 Olivart Pino⁴⁶ , M. Olocco¹⁹ , R.H. O'Neil⁵⁰ , J.S. Ordonez Soto¹¹ , D. Osthues¹⁹ ,
 J.M. Otalora Goicochea³ , P. Owen⁵² , A. Oyanguren⁴⁹ , O. Ozcelik⁵⁰ , F. Paciolla^{35,x} ,
 A. Padee⁴² , K.O. Padeken¹⁸ , B. Pagare⁴⁸ , T. Pajero⁵⁰ , A. Palano²⁴ , L. Palini³⁰ ,
 M. Palutan²⁸ , C. Pan⁷⁶ , X. Pan^{4,d} , S. Panebianco¹² , S. Paniskaki^{50,33} ,
 G. Panshin⁵ , L. Paolucci⁶⁴ , A. Papanestis⁵⁹ , M. Pappagallo^{24,i} , L.L. Pappalardo²⁶ ,
 C. Pappenheimer⁶⁷ , C. Parkes⁶⁴ , D. Parmar⁸⁰ , G. Passaleva²⁷ , D. Passaro^{35,t,50} ,
 A. Pastore²⁴ , M. Patel⁶³ , J. Patoc⁶⁵ , C. Patrignani^{25,k} , A. Paul⁷⁰ , C.J. Pawley⁸⁴ ,
 A. Pellegrino³⁸ , J. Peng^{5,7} , X. Peng⁷⁵ , M. Pepe Altarelli²⁸ , S. Perazzini²⁵ ,
 D. Pereima⁴⁴ , H. Pereira Da Costa⁶⁹ , M. Pereira Martinez⁴⁸ , A. Pereiro Castro⁴⁸ , C.
 Perez⁴⁷ , P. Perret¹¹ , A. Perrevoort⁸³ , A. Perro^{50,13} , M.J. Peters⁶⁷ , K. Petridis⁵⁶ ,
 A. Petrolini^{29,n} , S. Pezzulo^{29,n} , J. P. Pfaller⁶⁷ , H. Pham⁷⁰ , L. Pica^{35,t} ,
 M. Piccini³⁴ , L. Piccolo³² , B. Pietrzyk¹⁰ , G. Pietrzyk¹⁴ , R. N. Pilato⁶² ,
 D. Pinci³⁶ , F. Pisani⁵⁰ , M. Pizzichemi^{31,p,50} , V. M. Placinta⁴³ , M. Plo Casarus⁴⁸ ,
 T. Poeschl⁵⁰ , F. Polci¹⁶ , M. Poli Lener²⁸ , A. Poluektov¹³ , N. Polukhina⁴⁴ ,
 I. Polyakov⁶⁴ , E. Polycarpo³ , S. Ponce⁵⁰ , D. Popov^{7,50} , K. Popp¹⁹ ,
 S. Poslavskii⁴⁴ , K. Prasanth⁶⁰ , C. Prouve⁴⁵ , D. Provenzano^{32,l,50} , V. Pugatch⁵⁴ , A.
 Puicercus Gomez⁵⁰ , G. Punzi^{35,u} , J.R. Pybus⁶⁹ , Q. Q. Qian⁶ , W. Qian⁷ ,
 N. Qin^{4,d} , R. Quagliani⁵⁰ , R.I. Rabadan Trejo⁵⁸ , R. Racz⁸² , J.H. Rademacker⁵⁶ ,
 M. Rama³⁵ , M. Ramírez García⁸⁸ , V. Ramos De Oliveira⁷¹ , M. Ramos Pernas⁵⁸ ,
 M.S. Rangel³ , F. Ratnikov⁴⁴ , G. Raven³⁹ , M. Rebollo De Miguel⁴⁹ , F. Redi^{30,j} ,
 J. Reich⁵⁶ , F. Reiss²⁰ , Z. Ren⁷ , P.K. Resmi⁶⁵ , M. Ribalda Galvez⁴⁶ ,
 R. Ribatti⁵¹ , G. Ricart^{15,12} , D. Riccardi^{35,t} , S. Ricciardi⁵⁹ , K. Richardson⁶⁶ ,
 M. Richardson-Slipper⁵⁷ , F. Riehn¹⁹ , K. Rinnert⁶² , P. Robbe^{14,50} , G. Robertson⁶¹ ,
 E. Rodrigues⁶² , A. Rodriguez Alvarez⁴⁶ , E. Rodriguez Fernandez⁴⁸ ,
 J.A. Rodriguez Lopez⁷⁸ , E. Rodriguez Rodriguez⁵⁰ , J. Roensch¹⁹ , A. Rogachev⁴⁴ ,
 A. Rogovskiy⁵⁹ , D.L. Rolf¹⁹ , P. Roloff⁵⁰ , V. Romanovskiy⁶⁷ , A. Romero Vidal⁴⁸ ,
 G. Romolini^{26,50} , F. Ronchetti⁵¹ , T. Rong⁶ , M. Rotondo²⁸ , S. R. Roy²² ,
 M.S. Rudolph⁷⁰ , M. Ruiz Diaz²² , R.A. Ruiz Fernandez⁴⁸ , J. Ruiz Vidal⁸⁴ , J.
 J. Saavedra-Arias⁹ , J.J. Saborido Silva⁴⁸ , S. E. R. Sacha Emile R.⁵⁰ , N. Sagidova⁴⁴ ,
 D. Sahoo⁸¹ , N. Sahoo⁵⁵ , B. Saitta³² , M. Salomoni^{31,50,p} , I. Sanderswood⁴⁹ ,
 R. Santacesaria³⁶ , C. Santamarina Rios⁴⁸ , M. Santimaria²⁸ , L. Santoro² ,
 E. Santovetti³⁷ , A. Saputi^{26,50} , D. Saranin⁴⁴ , A. Sarnatskiy⁸³ , G. Sarpis⁵⁰ ,
 M. Sarpis⁸² , C. Satriano^{36,v} , A. Satta³⁷ , M. Saur⁷⁵ , D. Savrina⁴⁴ , H. Sazak¹⁷ ,
 F. Sborzacchi^{50,28} , A. Scarabotto¹⁹ , S. Schael¹⁷ , S. Scherl⁶² , M. Schiller²² ,
 H. Schindler⁵⁰ , M. Schmelling²¹ , B. Schmidt⁵⁰ , N. Schmidt⁶⁹ , S. Schmitt⁶⁶ ,
 H. Schmitz¹⁸ , O. Schneider⁵¹ , A. Schopper⁶³ , N. Schulte¹⁹ , M.H. Schune¹⁴ ,
 G. Schwering¹⁷ , B. Sciascia²⁸ , A. Sciuccati⁵⁰ , G. Scriven⁸⁴ , I. Segal⁸⁰ ,
 S. Sellam⁴⁸ , A. Semennikov⁴⁴ , T. Senger⁵² , M. Senghi Soares³⁹ , A. Sergi^{29,n} ,
 N. Serra⁵² , L. Sestini²⁷ , A. Seuthe¹⁹ , B. Sevilla Sanjuan⁴⁷ , Y. Shang⁶ ,
 D.M. Shangase⁸⁸ , M. Shapkin⁴⁴ , R. S. Sharma⁷⁰ , I. Shchemerov⁴⁴ , L. Shchutska⁵¹ ,
 T. Shears⁶² , L. Shekhtman⁴⁴ , Z. Shen³⁸ , S. Sheng^{5,7} , V. Shevchenko⁴⁴ , B. Shi⁷ ,
 Q. Shi⁷ , W. S. Shi⁷⁴ , Y. Shimizu¹⁴ , E. Shmanin²⁵ , R. Shorkin⁴⁴ ,
 J.D. Shupperd⁷⁰ , R. Silva Coutinho² , G. Simi^{33,r} , S. Simone^{24,i} , M. Singha⁸¹ ,
 N. Skidmore⁵⁸ , T. Skwarnicki⁷⁰ , M.W. Slater⁵⁵ , E. Smith⁶⁶ , K. Smith⁶⁹ ,
 M. Smith⁶³ , L. Soares Lavra⁶⁰ , M.D. Sokoloff⁶⁷ , F.J.P. Soler⁶¹ , A. Solomin⁵⁶ ,
 A. Solovov⁴⁴ , K. Solovieva²⁰ , N. S. Sommerfeld¹⁸ , R. Song¹ , Y. Song⁵¹ ,
 Y. Song^{4,d} , Y. S. Song⁶ , F.L. Souza De Almeida⁴⁶ , B. Souza De Paula³ ,

K.M. Sowa⁴⁰ , E. Spadaro Norella^{29,n} , E. Spedicato²⁵ , J.G. Speer¹⁹ , P. Spradlin⁶¹ ,
 F. Stagni⁵⁰ , M. Stahl⁸⁰ , S. Stahl⁵⁰ , S. Stanislaus⁶⁵ , M. Stefaniak⁸⁹ , E.N. Stein⁵⁰ ,
 O. Steinkamp⁵² , D. Strekalina⁴⁴ , Y. Su⁷ , F. Suljik⁶⁵ , J. Sun³² , J. Sun⁶⁴ ,
 L. Sun⁷⁶ , D. Sundfeld² , W. Sutcliffe⁵² , P. Svihra⁷⁹ , V. Svintozelskyi⁴⁹ ,
 K. Swientek⁴⁰ , F. Swystun⁵⁷ , A. Szabelski⁴² , T. Szumlak⁴⁰ , Y. Tan⁴ , Y. Tang⁷⁶ ,
 Y. T. Tang⁷ , M.D. Tat²² , J. A. Teijeiro Jimenez⁴⁸ , A. Terentev⁴⁴ , F. Terzuoli^{35,x} ,
 F. Teubert⁵⁰ , E. Thomas⁵⁰ , D.J.D. Thompson⁵⁵ , A. R. Thomson-Strong⁶⁰ ,
 H. Tilquin⁶³ , V. Tisserand¹¹ , S. T'Jampens¹⁰ , M. Tobin^{5,50} , T. T. Todorov²⁰ ,
 L. Tomassetti^{26,m} , G. Tonani³⁰ , X. Tong⁶ , T. Tork³⁰ , D. Torres Machado² ,
 L. Toscano¹⁹ , D.Y. Tou^{4,d} , C. Tripp⁴⁷ , G. Tuci²² , N. Tuning³⁸ , L.H. Uecker²² ,
 A. Ukleja⁴⁰ , D.J. Unverzagt²² , A. Upadhyay⁵⁰ , B. Urbach⁶⁰ , A. Usachov³⁸ ,
 A. Ustyuzhanin⁴⁴ , U. Uwer²² , V. Vagnoni^{25,50} , V. Valcarce Cadenas⁴⁸ ,
 G. Valenti²⁵ , N. Valls Canudas⁵⁰ , J. van Eldik⁵⁰ , H. Van Hecke⁶⁹ ,
 E. van Herwijnen⁶³ , C.B. Van Hulse^{48,aa} , R. Van Laak⁵¹ , M. van Veghel⁸⁴ ,
 G. Vasquez⁵² , R. Vazquez Gomez⁴⁶ , P. Vazquez Regueiro⁴⁸ , C. Vázquez Sierra⁴⁵ ,
 S. Vecchi²⁶ , J. Velilla Serna⁴⁹ , J.J. Velthuis⁵⁶ , M. Veltri^{27,y} , A. Venkateswaran⁵¹ ,
 M. Verdoglia³² , M. Vesterinen⁵⁸ , W. Vetens⁷⁰ , D. Vico Benet⁶⁵ , P.
 Vidrier Villalba⁴⁶ , M. Vieites Diaz⁴⁸ , X. Vilasis-Cardona⁴⁷ , E. Vilella Figueras⁶² ,
 A. Villa²⁵ , P. Vincent¹⁶ , B. Vivacqua³ , F.C. Volle⁵⁵ , D. vom Bruch¹³ ,
 N. Voropaev⁴⁴ , K. Vos⁸⁴ , C. Vrahas⁶⁰ , J. Wagner¹⁹ , J. Walsh³⁵ , E.J. Walton^{1,58} ,
 G. Wan⁶ , A. Wang⁷ , B. Wang⁵ , C. Wang²² , G. Wang⁸ , H. Wang⁷⁵ ,
 J. Wang⁶ , J. Wang⁵ , J. Wang^{4,d} , J. Wang⁷⁶ , M. Wang⁵⁰ , N. W. Wang⁷ ,
 R. Wang⁵⁶ , X. Wang⁸ , X. Wang⁷⁴ , X. W. Wang⁶³ , Y. Wang⁷⁷ , Y. Wang⁶ , Y. H.
 Wang⁷⁵ , Z. Wang¹⁴ , Z. Wang³⁰ , J.A. Ward^{58,1} , M. Waterlaet⁵⁰ , N.K. Watson⁵⁵ ,
 D. Websdale⁶³ , Y. Wei⁶ , Z. Weida⁷ , J. Wendel⁴⁵ , B.D.C. Westhenry⁵⁶ ,
 C. White⁵⁷ , M. Whitehead⁶¹ , E. Whiter⁵⁵ , A.R. Wiederhold⁶⁴ , D. Wiedner¹⁹ , M.
 A. Wiegertjes³⁸ , C. Wild⁶⁵ , G. Wilkinson^{65,50} , M.K. Wilkinson⁶⁷ , M. Williams⁶⁶ ,
 M. J. Williams⁵⁰ , M.R.J. Williams⁶⁰ , R. Williams⁵⁷ , S. Williams⁵⁶ , Z. Williams⁵⁶ ,
 F.F. Wilson⁵⁹ , M. Winn¹² , W. Wislicki⁴² , M. Witek⁴¹ , L. Witola¹⁹ , T. Wolf²² , E.
 Wood⁵⁷ , G. Wormser¹⁴ , S.A. Wotton⁵⁷ , H. Wu⁷⁰ , J. Wu⁸ , X. Wu⁷⁶ , Y. Wu^{6,57} ,
 Z. Wu⁷ , K. Wyllie⁵⁰ , S. Xian⁷⁴ , Z. Xiang⁵ , Y. Xie⁸ , T. X. Xing³⁰ , A. Xu^{35,t} ,
 L. Xu^{4,d} , M. Xu⁵⁰ , Z. Xu⁵⁰ , Z. Xu⁷ , Z. Xu⁵ , S. Yadav²⁶ , K. Yang⁶³ ,
 X. Yang⁶ , Y. Yang¹⁵ , Y. Yang⁸¹ , Z. Yang⁶ , V. Yeroshenko¹⁴ , H. Yeung⁶⁴ ,
 H. Yin⁸ , X. Yin⁷ , C. Y. Yu⁶ , J. Yu⁷³ , X. Yuan⁵ , Y. Yuan^{5,7} , J.
 A. Zamora Saa⁷² , M. Zavertyaev²¹ , M. Zdybal⁴¹ , F. Zenesini²⁵ , C. Zeng^{5,7} ,
 M. Zeng^{4,d} , C. Zhang⁶ , D. Zhang⁸ , J. Zhang⁷ , L. Zhang^{4,d} , R. Zhang⁸ ,
 S. Zhang⁶⁵ , S. L. Zhang⁷³ , Y. Zhang⁶ , Y. Z. Zhang^{4,d} , Z. Zhang^{4,d} , Y. Zhao²² ,
 A. Zhelezov²² , S. Z. Zheng⁶ , X. Z. Zheng^{4,d} , Y. Zheng⁷ , T. Zhou⁶ , X. Zhou⁸ ,
 Y. Zhou⁷ , V. Zhovkovska⁵⁸ , L. Z. Zhu⁷ , X. Zhu^{4,d} , X. Zhu⁸ , Y. Zhu¹⁷ ,
 V. Zhukov¹⁷ , J. Zhuo⁴⁹ , Q. Zou^{5,7} , D. Zuliani^{33,r} , G. Zunica²⁸ .

¹*School of Physics and Astronomy, Monash University, Melbourne, Australia*

²*Centro Brasileiro de Pesquisas Físicas (CBPF), Rio de Janeiro, Brazil*

³*Universidade Federal do Rio de Janeiro (UFRJ), Rio de Janeiro, Brazil*

⁴*Department of Engineering Physics, Tsinghua University, Beijing, China*

⁵*Institute Of High Energy Physics (IHEP), Beijing, China*

⁶*School of Physics State Key Laboratory of Nuclear Physics and Technology, Peking University, Beijing, China*

⁷*University of Chinese Academy of Sciences, Beijing, China*

⁸*Institute of Particle Physics, Central China Normal University, Wuhan, Hubei, China*

⁹*Consejo Nacional de Rectores (CONARE), San Jose, Costa Rica*

¹⁰*Université Savoie Mont Blanc, CNRS, IN2P3-LAPP, Annecy, France*

- ¹¹ *Université Clermont Auvergne, CNRS/IN2P3, LPC, Clermont-Ferrand, France*
- ¹² *Université Paris-Saclay, Centre d'Etudes de Saclay (CEA), IRFU, Saclay, France, Gif-Sur-Yvette, France*
- ¹³ *Aix Marseille Univ, CNRS/IN2P3, CPPM, Marseille, France*
- ¹⁴ *Université Paris-Saclay, CNRS/IN2P3, IJCLab, Orsay, France*
- ¹⁵ *Laboratoire Leprince-Ringuet, CNRS/IN2P3, Ecole Polytechnique, Institut Polytechnique de Paris, Palaiseau, France*
- ¹⁶ *Laboratoire de Physique Nucléaire et de Hautes Énergies (LPNHE), Sorbonne Université, CNRS/IN2P3, F-75005 Paris, France, Paris, France*
- ¹⁷ *I. Physikalisches Institut, RWTH Aachen University, Aachen, Germany*
- ¹⁸ *Universität Bonn - Helmholtz-Institut für Strahlen und Kernphysik, Bonn, Germany*
- ¹⁹ *Fakultät Physik, Technische Universität Dortmund, Dortmund, Germany*
- ²⁰ *Physikalisches Institut, Albert-Ludwigs-Universität Freiburg, Freiburg, Germany*
- ²¹ *Max-Planck-Institut für Kernphysik (MPIK), Heidelberg, Germany*
- ²² *Physikalisches Institut, Ruprecht-Karls-Universität Heidelberg, Heidelberg, Germany*
- ²³ *School of Physics, University College Dublin, Dublin, Ireland*
- ²⁴ *INFN Sezione di Bari, Bari, Italy*
- ²⁵ *INFN Sezione di Bologna, Bologna, Italy*
- ²⁶ *INFN Sezione di Ferrara, Ferrara, Italy*
- ²⁷ *INFN Sezione di Firenze, Firenze, Italy*
- ²⁸ *INFN Laboratori Nazionali di Frascati, Frascati, Italy*
- ²⁹ *INFN Sezione di Genova, Genova, Italy*
- ³⁰ *INFN Sezione di Milano, Milano, Italy*
- ³¹ *INFN Sezione di Milano-Bicocca, Milano, Italy*
- ³² *INFN Sezione di Cagliari, Monserrato, Italy*
- ³³ *INFN Sezione di Padova, Padova, Italy*
- ³⁴ *INFN Sezione di Perugia, Perugia, Italy*
- ³⁵ *INFN Sezione di Pisa, Pisa, Italy*
- ³⁶ *INFN Sezione di Roma La Sapienza, Roma, Italy*
- ³⁷ *INFN Sezione di Roma Tor Vergata, Roma, Italy*
- ³⁸ *Nikhef National Institute for Subatomic Physics, Amsterdam, Netherlands*
- ³⁹ *Nikhef National Institute for Subatomic Physics and VU University Amsterdam, Amsterdam, Netherlands*
- ⁴⁰ *AGH - University of Krakow, Faculty of Physics and Applied Computer Science, Kraków, Poland*
- ⁴¹ *Henryk Niewodniczanski Institute of Nuclear Physics Polish Academy of Sciences, Kraków, Poland*
- ⁴² *National Center for Nuclear Research (NCBJ), Warsaw, Poland*
- ⁴³ *Horia Hulubei National Institute of Physics and Nuclear Engineering, Bucharest-Magurele, Romania*
- ⁴⁴ *Authors affiliated with an institute formerly covered by a cooperation agreement with CERN.*
- ⁴⁵ *Universidad de Coruña, A Coruña, Spain*
- ⁴⁶ *ICCUB, Universitat de Barcelona, Barcelona, Spain*
- ⁴⁷ *La Salle, Universitat Ramon Llull, Barcelona, Spain*
- ⁴⁸ *Instituto Galego de Física de Altas Enerxías (IGFAE), Universidade de Santiago de Compostela, Santiago de Compostela, Spain*
- ⁴⁹ *Instituto de Física Corpuscular, Centro Mixto Universidad de Valencia - CSIC, Valencia, Spain*
- ⁵⁰ *European Organization for Nuclear Research (CERN), Geneva, Switzerland*
- ⁵¹ *Institute of Physics, Ecole Polytechnique Fédérale de Lausanne (EPFL), Lausanne, Switzerland*
- ⁵² *Physik-Institut, Universität Zürich, Zürich, Switzerland*
- ⁵³ *NSC Kharkiv Institute of Physics and Technology (NSC KIPT), Kharkiv, Ukraine*
- ⁵⁴ *Institute for Nuclear Research of the National Academy of Sciences (KINR), Kyiv, Ukraine*
- ⁵⁵ *School of Physics and Astronomy, University of Birmingham, Birmingham, United Kingdom*
- ⁵⁶ *H.H. Wills Physics Laboratory, University of Bristol, Bristol, United Kingdom*
- ⁵⁷ *Cavendish Laboratory, University of Cambridge, Cambridge, United Kingdom*
- ⁵⁸ *Department of Physics, University of Warwick, Coventry, United Kingdom*
- ⁵⁹ *STFC Rutherford Appleton Laboratory, Didcot, United Kingdom*
- ⁶⁰ *School of Physics and Astronomy, University of Edinburgh, Edinburgh, United Kingdom*
- ⁶¹ *School of Physics and Astronomy, University of Glasgow, Glasgow, United Kingdom*

- ⁶² *Oliver Lodge Laboratory, University of Liverpool, Liverpool, United Kingdom*
- ⁶³ *Imperial College London, London, United Kingdom*
- ⁶⁴ *Department of Physics and Astronomy, University of Manchester, Manchester, United Kingdom*
- ⁶⁵ *Department of Physics, University of Oxford, Oxford, United Kingdom*
- ⁶⁶ *Massachusetts Institute of Technology, Cambridge, MA, United States*
- ⁶⁷ *University of Cincinnati, Cincinnati, OH, United States*
- ⁶⁸ *University of Maryland, College Park, MD, United States*
- ⁶⁹ *Los Alamos National Laboratory (LANL), Los Alamos, NM, United States*
- ⁷⁰ *Syracuse University, Syracuse, NY, United States*
- ⁷¹ *Pontifícia Universidade Católica do Rio de Janeiro (PUC-Rio), Rio de Janeiro, Brazil, associated to ³*
- ⁷² *Universidad Andres Bello, Santiago, Chile, associated to ⁵²*
- ⁷³ *School of Physics and Electronics, Hunan University, Changsha City, China, associated to ⁸*
- ⁷⁴ *State Key Laboratory of Nuclear Physics and Technology, South China Normal University, Guangzhou, China., Guangzhou, China, associated to ⁴*
- ⁷⁵ *Lanzhou University, Lanzhou, China, associated to ⁵*
- ⁷⁶ *School of Physics and Technology, Wuhan University, Wuhan, China, associated to ⁴*
- ⁷⁷ *Henan Normal University, Xinxiang, China, associated to ⁸*
- ⁷⁸ *Departamento de Física , Universidad Nacional de Colombia, Bogota, Colombia, associated to ¹⁶*
- ⁷⁹ *Institute of Physics of the Czech Academy of Sciences, Prague, Czech Republic, associated to ⁶⁴*
- ⁸⁰ *Ruhr Universitaet Bochum, Fakultae f. Physik und Astronomie, Bochum, Germany, associated to ¹⁹*
- ⁸¹ *Eotvos Lorand University, Budapest, Hungary, associated to ⁵⁰*
- ⁸² *Faculty of Physics, Vilnius University, Vilnius, Lithuania, associated to ²⁰*
- ⁸³ *Van Swinderen Institute, University of Groningen, Groningen, Netherlands, associated to ³⁸*
- ⁸⁴ *Universiteit Maastricht, Maastricht, Netherlands, associated to ³⁸*
- ⁸⁵ *Tadeusz Kosciuszko Cracow University of Technology, Cracow, Poland, associated to ⁴¹*
- ⁸⁶ *Department of Physics and Astronomy, Uppsala University, Uppsala, Sweden, associated to ⁶¹*
- ⁸⁷ *Taras Schevchenko University of Kyiv, Faculty of Physics, Kyiv, Ukraine, associated to ¹⁴*
- ⁸⁸ *University of Michigan, Ann Arbor, MI, United States, associated to ⁷⁰*
- ⁸⁹ *Ohio State University, Columbus, United States, associated to ⁶⁹*
- ^a *Universidade Estadual de Campinas (UNICAMP), Campinas, Brazil*
- ^b *Centro Federal de Educação Tecnológica Celso Suckow da Fonseca, Rio De Janeiro, Brazil*
- ^c *Department of Physics and Astronomy, University of Victoria, Victoria, Canada*
- ^d *Center for High Energy Physics, Tsinghua University, Beijing, China*
- ^e *Hangzhou Institute for Advanced Study, UCAS, Hangzhou, China*
- ^f *LIP6, Sorbonne Université, Paris, France*
- ^g *Lamarr Institute for Machine Learning and Artificial Intelligence, Dortmund, Germany*
- ^h *Universidad Nacional Autónoma de Honduras, Tegucigalpa, Honduras*
- ⁱ *Università di Bari, Bari, Italy*
- ^j *Università di Bergamo, Bergamo, Italy*
- ^k *Università di Bologna, Bologna, Italy*
- ^l *Università di Cagliari, Cagliari, Italy*
- ^m *Università di Ferrara, Ferrara, Italy*
- ⁿ *Università di Genova, Genova, Italy*
- ^o *Università degli Studi di Milano, Milano, Italy*
- ^p *Università degli Studi di Milano-Bicocca, Milano, Italy*
- ^q *Università di Modena e Reggio Emilia, Modena, Italy*
- ^r *Università di Padova, Padova, Italy*
- ^s *Università di Perugia, Perugia, Italy*
- ^t *Scuola Normale Superiore, Pisa, Italy*
- ^u *Università di Pisa, Pisa, Italy*
- ^v *Università della Basilicata, Potenza, Italy*
- ^w *Università di Roma Tor Vergata, Roma, Italy*
- ^x *Università di Siena, Siena, Italy*
- ^y *Università di Urbino, Urbino, Italy*
- ^z *Universidad de Ingeniería y Tecnología (UTEC), Lima, Peru*
- ^{aa} *Universidad de Alcalá, Alcalá de Henares , Spain*